

# POLITECNICO DI MILANO

FACOLTÁ DI INGEGNERIA INDUSTRIALE

Corso di Laurea in Ingegneria Aeronautica



EXPERIMENTAL MEASUREMENT OF THE EFFICIENCY OF TURBULENT MIXING  
FOR NON-CONVENTIONAL MIXERS

**Relatore:**  
Prof. Maurizio Quadrio  
**Correlatore:**  
Prof. Pietro Poesio  
**Tutor:**  
Dott. Stefano Farisè

**Laureando:**  
Davide Arnone  
Matr.754872

Anno Accademico 2012-2013



*Alla mia famiglia  
Ai miei nipoti  
Ai miei amici*



# Contents

<b>Contents</b>	<b>i</b>
<b>List of Figures</b>	<b>iii</b>
<b>1 Introduzione</b>	<b>1</b>
1.1 L'importanza del mixing . . . . .	1
1.2 Motivazioni del lavoro di tesi . . . . .	2
<b>2 Percorso di ricerca</b>	<b>3</b>
<b>3 Introduction</b>	<b>7</b>
3.1 The importance of mixing . . . . .	7
3.2 Reasons of the research work . . . . .	7
3.3 Thesis structure . . . . .	8
<b>4 Preliminary studies</b>	<b>9</b>
4.1 Mixing . . . . .	9
4.1.1 Mixer for liquids . . . . .	9
4.1.2 Experimental tests on mixers . . . . .	11
4.1.3 Dimensionless numbers . . . . .	12
4.2 Theory of heat transfer in semi-infinite plane . . . . .	14
<b>5 Experimental Setup</b>	<b>19</b>
5.1 Design choises . . . . .	19
5.2 3D model . . . . .	20
5.3 Configurations of the mixer . . . . .	21
5.4 Power supply . . . . .	22
5.5 Heating and cooling system . . . . .	22
5.6 Motor . . . . .	22
5.7 Sensors . . . . .	24
5.7.1 Thermocouples . . . . .	24
5.7.2 Current sensor . . . . .	24
5.7.3 Encoder . . . . .	25
5.8 Acquisition system . . . . .	26

5.8.1	LabVIEW . . . . .	26
5.8.2	NI USB-6009 . . . . .	27
5.8.3	NI9213 and NI9205 . . . . .	27
5.9	Matlab . . . . .	29
5.9.1	Post-process of temperature data . . . . .	29
5.9.2	Post-process of motor data . . . . .	30
5.10	Experimental Procedure . . . . .	32
5.11	Diagram of the experimental setup . . . . .	33
<b>6</b>	<b>Validation</b>	<b>35</b>
6.1	Test of the thermocouples . . . . .	35
6.2	Cooling test . . . . .	41
6.3	Heating test . . . . .	41
6.4	Mixing time procedure test . . . . .	44
6.5	Test of the experimental procedure . . . . .	47
6.6	Calibration of the current sensor . . . . .	48
6.7	Estimation errors . . . . .	49
<b>7</b>	<b>Experimental Data</b>	<b>51</b>
7.1	Case 1: free slinky+ . . . . .	51
7.2	Case 2: free slinky- . . . . .	55
7.3	Case 3: fixed slinky . . . . .	59
7.4	Case 4: impeller . . . . .	63
7.5	Comparison . . . . .	67
<b>8</b>	<b>Conclusions</b>	<b>71</b>
8.1	Achievements . . . . .	71
8.2	Future developments . . . . .	72
	<b>Notations</b>	<b>74</b>
	<b>Bibliography</b>	<b>76</b>

# List of Figures

4.1	Viscosity ranges for different impellers . . . . .	10
4.2	Flow field for axial impeller (a) and for radial impeller (b) . . . . .	11
4.3	Example of homogenization . . . . .	12
4.4	Error function . . . . .	16
4.5	Theoretical temperature distribution in the cylinder at $t=0$ . . . . .	16
4.6	Theoretical temperature distribution in the cylinder at $t=1800s$ . . . . .	17
4.7	Theoretical temperature at $t=[0,1800,3600,7200]s$ . . . . .	17
5.1	3D model of the mixer . . . . .	20
5.2	Slinky spring mounted on the shaft . . . . .	21
5.3	Programmable DC power supply Agilent E3631A . . . . .	22
5.4	Particular of the heat exchanger under the mixer . . . . .	23
5.5	View of the heat exchanger under the mixer . . . . .	23
5.6	Metal Gearmotor 37Dx52L mm . . . . .	23
5.7	View of thermocouples . . . . .	24
5.8	Current sensor ACS712 . . . . .	25
5.9	Example of encoder square wave output [3.65rps] . . . . .	25
5.10	Screenshot of LabVIEW virtual instrument . . . . .	26
5.11	Low-Cost Multifunction DAQ NI USB-6009 . . . . .	27
5.12	Thermocouple Input Module NI9213 . . . . .	28
5.13	Voltage Input Module NI9205 . . . . .	28
5.14	Example of total graph of a test [3.65rps] . . . . .	29
5.15	Example of mixing graph of a test [3.65rps] . . . . .	30
5.16	Example of original current data of a test [3.65rps] . . . . .	31
5.17	Example of locating the beginning of the mixing [3.65rps] . . . . .	31
5.18	Example of power on rps graph . . . . .	31
5.19	Diagram of the experimental setup . . . . .	33
6.1	$\Delta T_i^f$ for three tests at 3.65rps . . . . .	35
6.2	Maximum value of variation $\Delta T_i^f$ for three tests at 3.65rps . . . . .	36
6.3	$\Delta T_i^f$ for three tests at 3.65rps with different configurations . . . . .	36
6.4	Maximum value of variation $\Delta T_i^f$ for three tests at 3.65rps with different configurations . . . . .	37

6.5	$\Delta T_i^f$ for three tests at [0.53,1.79,7.94] <i>rps</i> . . . . .	37
6.6	Maximum value of variation $\Delta T_i^f$ for three tests at [0.53,1.79,7.94] <i>rps</i> . . . . .	38
6.7	$\Delta T_i^f$ for three tests at different velocities with different configurations . . . . .	38
6.8	Maximum value of variation $\Delta T_i^f$ for three tests at different velocities with different configurations . . . . .	39
6.9	$\Delta T_i^{tot}$ between $T_a^i$ and $T_a^f$ . . . . .	40
6.10	Maximum value of variation $\Delta T_i^{tot}$ between $T_a^i$ and $T_a^f$ . . . . .	40
6.11	Stratification of the water with the cooling system . . . . .	41
6.12	Stratification using the theory of heat transfer in semi-infinite plane . . . . .	42
6.13	Stratification of the water with the heating system . . . . .	42
6.14	Stratification of the water using the theory of heat transfer in semi-infinite plane with hot wall . . . . .	43
6.15	Mixing time (a) using classical definition . . . . .	44
6.16	Mixing time (b) using classical definition . . . . .	44
6.17	Absolute value of the derivative of the temperatures . . . . .	45
6.18	Mixing time (a) using <i>STD</i> method . . . . .	46
6.19	Mixing time (b) using <i>STD</i> method . . . . .	46
6.20	Example of a test of 30 minutes of heating . . . . .	47
6.21	Another example of a test of 30 minutes of heating . . . . .	47
6.22	Current on <i>rps</i> for free slinky+ . . . . .	48
7.1	$t_m$ of slinky+ . . . . .	52
7.2	Logarithmic graph of $t_m$ of slinky+ . . . . .	53
7.3	Electric power consumption of slinky+ . . . . .	53
7.4	Energy consumption of slinky+ . . . . .	54
7.5	$t_m$ for slinky- . . . . .	56
7.6	Logarithmic graph of $t_m$ of slinky- . . . . .	56
7.7	Electric power consumption of slinky- . . . . .	57
7.8	Energy consumption of slinky- . . . . .	57
7.9	$t_m$ for fixed slinky . . . . .	60
7.10	Logarithmic graph of $t_m$ of fixed slinky . . . . .	60
7.11	Electric power consumption of fixed slinky . . . . .	61
7.12	Energy consumption of fixed slinky . . . . .	61
7.13	$t_m$ for impeller . . . . .	64
7.14	Logarithmic graph of $t_m$ for impeller . . . . .	64
7.15	Electric power consumption of impeller . . . . .	65
7.16	Energy consumption of impeller . . . . .	65
7.17	Comparison of $t_m$ . . . . .	67
7.18	Logarithmic graph of comparison of $t_m$ . . . . .	68
7.19	Comparison of electric power consumption . . . . .	68
7.20	Comparison of energy consumption . . . . .	69



## Abstract

Mixing is currently seeing a growing interest from many scientific and industrial sectors. The variety and complexity of the mixing in industrial applications requires careful selection and design to ensure an effective and efficient mixing. This research propose an unconventional configuration of turbulent mixer. This configuration aims to improve the mixing inside a cylindrical container using a twisted slinky spring instead of an impeller as in the classical design. During the rotation the spring is free to move axially compressing and relaxing since it is connected only at the two ends. In this way we want to reduce the drag associate with the mixing increasing it efficiency. We developed an experimental setup to measure the time required for the complete mixing and the electrical power absorbed by an electrical motor as a function of the rotation speed. We used a resistor placed in the upper layer of the cylinder to heat the liquid only by conduction and we acquired the temperature of twenty-six thermocouples placed along the height of the mixer. We imposed the desired variation of the average temperature in the cylinder to fix the amount of energy to mix into the system. We tested three different configurations: free spring, fixed spring, classic propeller. The results of the experiments are satisfactory. For each configuration the correlation between the mixing time and the rotational speed is in agreement with the literature. The configuration with the propeller presents mixing times lower but an electric power consumption higher than the one with spring. While in terms of energy consumption, the propeller system is efficient only at low speed, the spring is more efficient at high speed.

**Keywords:** mixer, turbulent-mixing, slinky spring, mixing time



## Sommario

Attualmente il mixing sta vedendo un crescente interesse da parte di numerosi settori scientifici ed industriali. La varietà e la complessità sempre crescente dei processi di miscelazione incontrati nelle applicazioni industriali richiede un'attenta selezione e progettazione per garantire un mixing efficace ed efficiente. Questo lavoro di ricerca propone lo studio di una configurazione non convenzionale di mixer turbolento. Tale configurazione prevede il mixing all'interno di un contenitore cilindrico per opera di una molla slinky al posto di una classica girante. Durante la rotazione, la molla, ritorta e vincolata agli estremi all'albero di rotazione, è libera di muoversi assialmente comprimendosi e distendendosi. In questo modo abbiamo cercato di ridurre la resistenza legata al mixing per renderlo più efficiente. Per qualificare questa configurazione di mixer si è sviluppato un setup sperimentale per misurare il tempo di miscelamento e la potenza elettrica assorbita in funzione della velocità di rotazione. Si è deciso di adottare un sistema basato sulla misurazione della temperatura disponendo ventisei termocoppie lungo tutta l'altezza del mixer. Tramite una resistenza posta nello strato superiore del cilindro è stato possibile riscaldare il liquido per sola conduzione. Imponendo la variazione desiderata di temperatura media nel cilindro è stata fissata la quantità di energia immessa nel sistema. Le prove sono state effettuate per diverse configurazioni (tutte non ottimizzate): molla libera, molla vincolata, elica. I risultati degli esperimenti risultano soddisfacenti. Per ogni configurazione l'andamento del tempo di miscelamento in funzione della velocità di rotazione è di tipo logaritmico in accordo con la letteratura. La configurazione munita di elica presenta tempi di miscelamento inferiori ma consumi in termini di potenza elettrica superiori rispetto a quella con la molla. In termini di energia spesa, adottando l'elica il sistema risulta efficiente alle basse velocità, usando la molla lo è alle alte.

**Parole chiave:** mixer, mixing turbolento, molla slinky, tempo di miscelamento



# Chapter 1

## Introduzione

### 1.1 L'importanza del mixing

Attualmente il mixing come disciplina sta vedendo un crescente interesse da parte di numerosi settori scientifici ed industriali. Per quanto lo studio di tale fenomeno possa presentare numerose difficoltà i potenziali vantaggi legati ad una sua migliore comprensione stanno spingendo la ricerca.

Il mixing risulta essere il centro della maggior parte dei sistemi di produzione industriali come quelli chimici, farmaceutici o alimentari e ricopre lo stesso ruolo in altri campi più specifici come ad esempio in numerosi macchinari medici o nell'ambito delle biotecnologie.

Che si tratti di miscelare due o più liquidi, liquidi e solidi, gas e liquidi e così via, dal processo di mixing dipendono la qualità e le caratteristiche dei prodotti ottenuti. Nonostante molte operazioni industriali richiedano requisiti di miscelazione facilmente ottenibili, sfruttando delle correlazioni note, ve ne sono molte altre che richiedono una valutazione più approfondita. Il costo di uno sviluppo mirato risulta essere inferiore rispetto al costo di adeguamento di un sistema sviluppato in modo errato e presenta un notevole potenziale economico. Numerosi studi hanno dimostrato quanto possano essere ingenti le perdite legate ad un poco efficiente mixing, si pensi che nel solo settore chimico americano nel 1989 tali perdite sono state stimate tra il miliardo e i 10 miliardi di dollari[3].

La varietà e la sempre crescente complessità dei processi di miscelazione incontrati nelle applicazioni industriali richiede un'attenta selezione e progettazione per garantire un mixing efficace ed efficiente. I moderni sistemi produttivi per essere competitivi necessitano di apparecchiature capaci di più rapidi tempi di miscelazione, di un consumo inferiore di potenza e di adattabilità per poter essere usati per prodotti differenti. Un mixer non è più un generico strumento di produzione ma uno strumento di lavoro fondamentale e decisivo.

## 1.2 Motivazioni del lavoro di tesi

La ricerca scientifica sul mixing procede lungo due strade principali: lo studio ed il miglioramento dei sistemi già esistenti e lo sviluppo di nuovi. Lungo questa seconda via è stato sviluppato il lavoro di tesi di F. Pasqua [9] nel quale è stata eseguita una prima analisi sperimentale di un mixer non convenzionale. Quest'ultimo è assimilabile ad un qualsiasi mixer per liquidi, dotato di contenitore cilindrico, con la particolarità di adottare una molla slinky al posto di una classica girante.

La molla slinky è stata ritorta e vincolata all'albero. Una volta azionato il mixer la molla comincia a ruotare e raggiunta una certa velocità di rotazione comincia a muoversi in direzione assiale comprimendosi e distendendosi. Si è ipotizzato che la continua modifica della forma della molla riesca ad influenzare positivamente il mixing.

I parametri da misurare per verificare la suddetta ipotesi sono di non facile individuazione. Il tempo di miscelamento, la potenza richiesta, il consumo energetico, il grado di miscelamento sono alcune delle molteplici prestazioni di un sistema di mixing. In questo lavoro di tesi è stato realizzato un nuovo mixer rispetto a quello studiato da Pasqua e si è sviluppata una procedura sperimentale per misurarne il tempo di miscelamento e la potenza elettrica richiesta.

## Chapter 2

# Percorso di ricerca

Lo scopo di questo lavoro di tesi è di effettuare delle misure sul mixing turbolento per qualificare le caratteristiche di un mixer non convenzionale nel quale viene usata una molla slinky come elemento rotante. Esistono svariati elementi per qualificare un sistema di mixing: il tempo di miscelamento, il consumo energetico, il consumo di potenza e così via. Il primo obiettivo del lavoro è stata la scelta del tipo di dati da misurare. Sono stati scelti il tempo di miscelamento ed il consumo di potenza. Oltre a tre configurazioni con la molla, ne abbiamo studiata anche una più classica utilizzando un'elica.

Non è possibile parlare di tempo di miscelamento in termini assoluti poiché va calcolato in funzione del grado di omogeneità che si vuole ottenere. Tipicamente si ricerca il tempo necessario per ottenere un'omogeneizzazione al 95% cioè l'istante di tempo oltre il quale la misura rimane tra il 95% ed il 105% del valore finale. Il valore attribuito al grado desiderato risulta essere funzione del tipo di impiego che si sta facendo del mixer.

Esistono diversi tipi di prove: basate sulla lettura di sensori oppure su metodi di visualizzazione. In questo lavoro abbiamo effettuato delle prove basate su misure di temperatura. Variando la temperatura nel mixer ed azionandolo si può ottenere il tempo di miscelamento analizzando i dati acquisiti. Abbiamo dotato il setup di un numero elevato di termocoppie per poter avere informazioni lungo tutta l'altezza del cilindro. Per variare la temperatura si è previsto un sistema di raffreddamento del fondo tramite un bagno termostato.

L'altro parametro che abbiamo deciso di misurare è la potenza elettrica consumata. Questo dato è facilmente calcolabile poiché è il prodotto tra corrente e tensione di alimentazione del motore. La tensione è nota in quanto regolata sull'alimentatore. Per misurare la corrente ci siamo serviti di un sensore. Ovviamente, ponendoci a questo livello, il consumo non è esattamente quello necessario al solo mixing ma risulta maggiorato da contributi esterni.

Per validare la scelta di raffreddare il fondo si è studiata la soluzione analitica per lo scambio termico in un corpo bidimensionale semi-infinito. Tale teoria permette di calcolare la distribuzione nello spazio e l'andamento nel tempo della temperatura in un corpo di estensione semi-infinita a contatto con una parete al-

la temperatura  $T_w$ . Già da queste prime prove teoriche si è capito che l'idea di raffreddare il fondo, pur evitando moti convettivi nell'acqua, avrebbe comportato notevoli svantaggi in termini di tempo.

Abbiamo modellato il mixer mediante il software SolidWork. Il setup progettato è costituito dal mixer, da un sistema di alimentazione, da ventisette termocoppie, da un encoder, da un sensore di corrente, da un sistema di acquisizione dati<sup>1</sup> e da una copertura in materiale isolante<sup>2</sup>.

Il sistema durante le prove acquisisce le termocoppie a  $3Hz$  per l'intera durata della prova. I dati relativi al motore, cioè corrente ed encoder, vengono acquisiti a  $1KHz$ . Per evitare che i file contenenti i dati acquisiti dal motore siano eccessivamente grandi la loro acquisizione avviene nei primi istanti di tempo e dopo il suo avvio. In tutta la fase intermedia non viene acquisito alcun dato. Il salvataggio degli istanti iniziali è essenziale per riuscire a ricavare il momento in cui viene acceso il motore. Questo istante viene considerato come inizio del mixing.

Si è eseguita una prova di stratificazione totale dell'acqua registrando un tempo superiore alla decina di ore. Si è poi azionato il mixer individuando un tempo di miscelamento di poche decine di secondi. Dovendo testare il mixer per molte condizioni differenti si è pensato di modificare il sistema in modo da permettere dei tempi di realizzazione prove più brevi. Con la stratificazione avremmo avuto il vantaggio di poter imporre facilmente le condizioni iniziali di ogni test pagando lo scotto di prove molto lunghe. Abbiamo quindi implementato un sistema di riscaldamento<sup>3</sup> da porre al di sotto del tappo del mixer. In questo modo siamo stati in grado di far variare in poco tempo ed in modo sostanziale la temperatura dell'acqua per sola conduzione. Si è subito notato che riscaldando il sistema, si potevano ottenere rapidi cambiamenti degli strati superiori già dopo pochi minuti. Si è ipotizzato che a differenza del sistema di raffreddamento, con il riscaldamento si possano raggiungere differenze di temperatura, tra parete e acqua, molto grandi. Per completezza si è studiato il caso del riscaldamento sfruttando la soluzione analitica.

Si è quindi iniziato un processo iterativo per individuare il metodo per calcolare il tempo di miscelamento e la procedura da attuare per avere prove con le medesime condizioni di pre-mixing. Dopo svariati test abbiamo individuato le seguenti procedure.

In quella numerica per la misura del tempo di miscelamento abbiamo analizzato la derivata delle temperature, calcolata tramite differenze finite. La derivata di tutte le temperature risulta molto piccola ma ha delle importanti variazioni nell'intervallo di tempo in cui avviene il miscelamento. Una volta individuato il suo massimo, in valore assoluto, muovendosi in avanti sull'asse dei tempi si è cercato l'istante nel quale il massimo della deviazione standard diventava minore di 0.0005, valore corrispondente ad un grado di omogeneità di circa il 98%.

---

<sup>1</sup>schede della NI e un computer con LabVIEW

<sup>2</sup>removibile

<sup>3</sup>costituito da una resistenza



Abbiamo definito la *STD* come:

$$\sigma_i(t) = \left( \frac{T_i(t) - (T_i^f - T_a^f)}{T_a(t)} - 1 \right)^2 \quad (2.1)$$

Per lo sviluppo di una procedura standard di prova ci siamo basati sulla considerazione che fosse necessario imporre le quantità di sostanze da miscelare, nel nostro caso acqua ed energia. Poichè all'interno del cilindro vi è sempre la stessa quantità di acqua e di questa conosciamo l'andamento nel tempo della temperatura di ogni suo strato, risulta possibile calcolare la quantità di energia ceduta al sistema:

$$Q(t) = \sum_1^{27} m_i \cdot c \cdot (T_i(t) - T_i^i) = 27 \cdot c \cdot m \cdot \Delta T_a(t) \quad (2.2)$$

Per le nostre prove abbiamo fissato un  $\Delta T_a$  di  $1.5^\circ C$ . Usando questo valore tutte le prove hanno una durata di circa 30 minuti.

Una volta affinate la procedura per gli esperimenti ed il metodo per valutare il tempo di miscelamento abbiamo iniziato la campagna di test.

Lo scopo del lavoro è di qualificare il mixer in base alla velocità per poter successivamente comparare le diverse configurazioni. Non abbiamo usato la tensione di alimentazione né la potenza elettrica poiché il dato relativo alla velocità risulta essere il più accurato. L'uscita dell'encoder è un'onda quadra. Valutando il tempo che intercorre tra una cresta e l'altra, è possibile ricavare la velocità in *rps*. Il sensore viene acquisito a  $1KHz$  perciò è in grado di leggere in modo accurato tutte le velocità raggiungibili dal mixer.

Per ogni test si è sempre applicata la medesima procedura: verificare la velocità di rotazione prima di collegare il sistema di riscaldamento in modo da impostare il giusto valore sull'alimentatore; nella condizione di acqua ferma collegare la resistenza; aspettare che il  $\Delta T_a$  arrivi a  $1.5^\circ C$ ; scollegare la resistenza e rimuoverla dall'acqua; accendere il motore.

La prima configurazione studiata è stata la molla libera in rotazione antioraria. Come ipotizzato il suo moto presenta differenti caratteristiche in base alla velocità di rotazione. Alle basse velocità ricorda una girante elicoidale poiché ruota solamente. Alle alte si concentra vicino al suo estremo inferiore. Per gli altri valori di velocità ruota e si muove assialmente. Il tempo di miscelamento presenta un andamento logaritmico. Ciò significa che alle basse velocità il mixer non riesce a miscelare bene. Incrementando la velocità il tempo di miscelamento arriva ad un valore asintotico di circa  $14s$  mentre il consumo di potenza cresce linearmente. Moltiplicando questi due valori abbiamo ottenuto il consumo elettrico del mixer. Il suo andamento è molto particolare infatti presenta tre minimi di cui due relativi.

Ultimati i test sulla slinky+ siamo passati alla slinky- adottando le medesime procedure ed usando i dati di velocità dei test precedenti come riferimento. A differenza della slinky+, in questo caso alle alte velocità la molla si concentra verso l'estremo più alto. Tempo di miscelamento e consumo energetico hanno

andamento simile alla configurazione precedente. Il consumo energetico ha ancora tre minimi ma molto ravvicinati tra loro.

Finiti i test con la molla libera, la abbiamo vincolata all'albero in modo da impedire qualsiasi movimento in direzione assiale. Con questa configurazione il mixer assomiglia molto di più ad alcuni mixer già esistenti. A differenza delle configurazioni precedenti si riscontra un peggioramento delle caratteristiche generali del mixer.

Come configurazione classica di confronto è stata presa una girante assiale. Il tempo di miscelamento ha anche per questa configurazione un andamento logaritmico. Il consumo di potenza non è più lineare ma esponenziale rispetto alla velocità, probabilmente a causa della resistenza idrodinamica. Anche il consumo energetico cresce esponenzialmente con la velocità.

Confrontando le diverse configurazioni del mixer è possibile trarre alcuni importanti considerazioni. In termini energetici la molla vincolata consuma più dei casi in cui è libera di muoversi assialmente. Ciò è dovuto ai maggiori tempi di miscelamento ed al maggior consumo di potenza elettrica. Comparando poi le tre configurazioni slinky con la girante, quest'ultima risulta più efficace ed efficiente alle basse velocità. Alle alte essa rimane efficace, in termini di tempo, ma risulta molto meno efficiente.

I risultati ottenuti sono stati molto soddisfacenti e presagiscono la possibilità di uno studio più approfondito di questo tipo di mixer. Interessante è il dato relativo al consumo di potenza elettrica il quale potrebbe suggerire un minore danneggiamento meccanico del fluido. Occorrerà quindi cercare di comprendere meglio le dinamiche all'interno del mixer.

# Chapter 3

## Introduction

### 3.1 The importance of mixing

Mixing, as a discipline, is currently seeing a growing interest by many scientific and industrial sectors. This is a complex phenomenon but the potential benefits of a better understanding are pushing research.

Mixing plays a key role in of most of the industrial production systems such as chemical, pharmaceutical or food and it is very important in other specific fields such as in medical equipments or in biotechnology.

Whether it is mixing of two or more liquids, liquids and solids, gases and liquids the quality and the properties of the products obtained depend on the mixing process. Although there are many industrial operations in which mixing requirements are readily scaled-up from known correlations, many operations require a more careful evaluation. The cost of a targeted development is smaller than the cost of adapting a system developed inaccurately and has great economic potential. Numerous studies demonstrated that losses due to poor-mixing can be huge. In 1989, the cost of poor mixing was estimated at \$1 billion to \$10 billion only in the U.S. chemical industry [3].

The wide variety and ever increasing complexity of mixing processes encountered in industrial applications requires careful selection, design and scale up to ensure effective and efficient mixing. Today's competitive production systems need robust equipment that has to be capable of faster blend times, lower power consumption and adaptability for use with multiple products. A mixer is no longer a generic production tool, but a critical and decisive business tool.

### 3.2 Reasons of the research work

Scientific research on mixing proceeds along two main paths: study and improvement of existing systems and development new ones. Following this second path the thesis work of F. Pasqua[9] has been developed. In this work was made a first experimental analysis of an unconventional mixer. This mixer had a cylindrical

container as any other mixer for liquids but it used a slinky spring instead of a classical impeller.

The spring is twisted and fixed to the rotational shaft. During rotation it is free to move axially compressing and relaxing. It has been speculated that the continuous change in its shape is able to positively influence the mixing.

It is not easy to find the parameters needed to prove this hypothesis. Mixing time, electric power consumption, energy consumption, degree of mixing are some of the many characteristics of this complex system. In this thesis we created a new mixer <sup>1</sup> and we developed an experimental procedure to measure mixing time and electrical power consumption.

### 3.3 Thesis structure

The outline of the thesis is as follows. In Chapter 3 we introduce the research area and the aim of this work. In Chapter 4 we review the preliminary studies that preceded the design of the experimental setup. In Chapter 5 we describe the experimental setup starting from the design to the acquisition system. Chapter 6 shows all the tests made to validate the experimental setup including the estimation of errors. In Chapter 7 we present the experimental data of the work. First each configuration and then the comparison between all of them. Chapter 8 contains the conclusions of this research and shows the possible future developments.

---

<sup>1</sup>new compared to the one studied by Pasqua

# Chapter 4

## Preliminary studies

### 4.1 Mixing

We define mixing a physical process which aims at reducing inhomogeneity in fluids to achieve a desired process result by eliminating gradients of concentration, temperature, and other properties. Liquid mixing and other mixing operations concerning a dispersed phase in a liquid are a common processes in the chemical and pharmaceutical manufacturing industry. These operations are usually carried out in glass-lined, stirred, torispherical-bottomed reactors.

#### 4.1.1 Mixer for liquids

Mixers for liquids can, usually, be classified according to the viscosity of the substances which need to be mixed (fig. 4.1)[8]. Mixing impellers are designed to produce *turbulence* and *pump* fluid. For mixing both of these elements are essential. They produce *fluid shear* and *fluid velocity* respectively. It is necessary that the fluid agitated by the impeller sweeps the entire tank in a sensible time and be sufficient to reach the most remote parts of the vessel. Fluid velocity also prevents solids sedimentation and produces flow over heating or cooling coils when necessary. Fluid shear means turbulent eddies. These are essential to micro-mixing. Mixing is certain to be inefficient unless flow in tank is turbulent. A good mixing could be described as a combination of three physical process : distribution, dispersion and diffusion.

- *Distribution* is dispersion of materials caused by bulk motion. It is often the slowest step in mixing process.
- *Dispersion* is the act of spreading out. Dispersion breaks up bulk flow into smaller and smaller eddies.
- *Turbulent diffusion* is dispersion in turbulent flows caused by the motions of eddies.
- *Molecular diffusion* is diffusion caused by relative molecular motion.

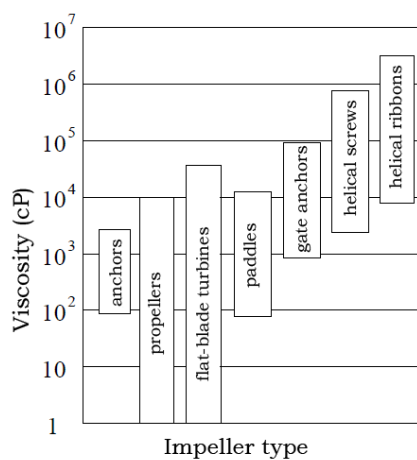


Figure 4.1: Viscosity ranges for different impellers

Distribution, dispersion and diffusion are related to different scales of mixing: macromixing, mesomixing and micromixing. The first is the slowest step. The last is the fastest.

All mixing impellers produce both fluid velocity and fluid shear, but different types of impellers produce different degrees of flow and turbulence, either of which may be important, depending on the application.

The choice of a mixer for a particular application depends on numerous process factors, some of which are:

- Type of application
- Viscosity
- Tank geometry
- Retention time and/or blend time

In this thesis we mixed only water so we focused on mixers equipped with propellers or turbines. Mixing impellers can be divided into two general categories: radial flow or axial flow. These two configurations generate different flow fields (fig. 4.2).

**Radial** flow impellers have multiple flat blades that are mounted parallel to the axis of the mixing shaft. Typical uses of these instruments are gas/liquid dispersion, liquid/liquid dispersion, flash mixing and low level mixing applications. If high shear is required, radial flow impellers should be preferred.

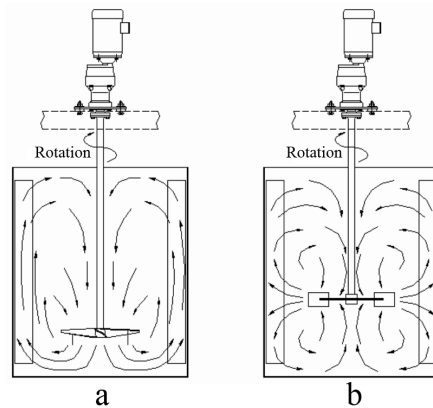


Figure 4.2: Flow field for axial impeller (a) and for radial impeller (b)

**Axial** flow impellers have blades which make an angle of less than  $90^\circ$  with the mixing shaft axis. Typical applications include simple blending, solids suspension and flocculation. Applications requiring high flow are generally best performed with axial flow impellers.

#### 4.1.2 Experimental tests on mixers

The aim of a mixer is to reduce degree of inhomogeneity of the substances present inside it. Once it is established the desired degree of homogeneity it is possible to define all the characteristics that qualify a system of mixing.

To perform a test it is necessary to establish two elements: quantity of substances that have to be mixed and degree of mixing that you want to achieve. By using collected data it is possible to identify the necessary mixing time to achieve the desired degree of homogeneity (fig. 4.3).

Once known the generated flow field, you can choose which regions are the best to perform measurements. For example we can have a poor mixing region. If you want to calculate mixing time conservatively, you need to measure in this region. Measurements of other regions may give a wrong value of calculated mixing time.

There are many kind of tests to qualify a mixer. They vary according to the substances which need to be mixed. For example you can perform conductivity measurements like Fort in [11] and [4]. You can also use the Schlieren effect to highlight the different density of the liquid. For a visual test you can introduce a tracer into the mixer and then analyse the captured images (for instance Busciglio et al. in [1]). In case of opaque liquids you can use temperature sensors.

Every type of test do not have to alter the characteristics of the substances that are mixed. For example in case of temperature tests you need to operate in a range of temperatures in which viscosity of the mixed liquid does not change. Another essential request is that measuring instruments must not be too invasive to avoid excessively modifications of the flow field.

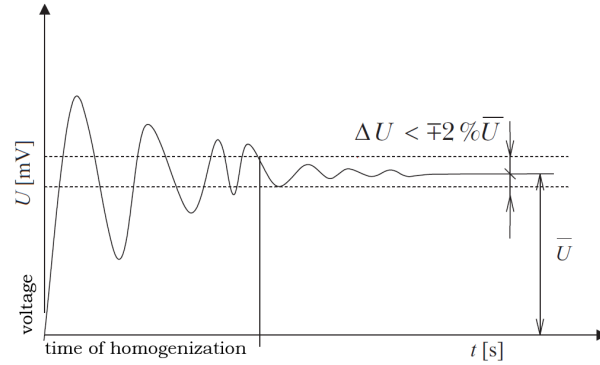


Figure 4.3: Example of homogenization

### Processing mixing time data

Data collected by the conductivity (Fort in [11]), thermocouple or pH techniques must be processed to obtain mixing time for the system that is under investigation. Data must be first normalized to eliminate the effect of different probe gains. Data are normalized between an initial value of zero that is measured before adding tracer, and a final stable value measured after test is completed. The normalized output is obtain by

$$C'_i = \frac{C_i - C_0}{C_\infty - C_0} \quad (4.1)$$

where  $C'_i$  is normalized probe output. Mixing time is defined as time that normalized probe output needs to reach and remain between 95 and 105% ( $\pm 5\%$ ) of the final equilibrium value.

#### 4.1.3 Dimensionless numbers

To compare different mixers is useful to define some dimensionless numbers. For mixing tanks the Reynolds number is defined as

$$Re = \frac{\rho N D^2}{\mu} \quad (4.2)$$

where  $\rho$  is the fluid density,  $D$  is the impeller diameter,  $N$  is the impeller speed (in *rps*) and  $\mu$  is the dynamic viscosity.

The power number is a dimensionless parameter that provides a measure of the power requirements for the operation of an impeller. It is defined a

$$N_p = \frac{P}{\rho N^3 D^5} \quad (4.3)$$

Another number is the dimensionless mixing time that is defined as

$$N_t = N * t_m \quad (4.4)$$



$N_t$  can be considered as the number of complete rounds of the impeller to reach the desired value of homogeneity.

With our mixer we can use only the definition of dimensionless mixing time because of the impossibility to set a value of  $D$  for the slinky.

## 4.2 Theory of heat transfer in semi-infinite plane

We used [6] as reference. We have a bi-dimensional semi-infinite region. One boundary, initially at  $T = T_0$ , is suddenly cooled (or heated) at a new temperature,  $T_\infty$ .

General functions that we are going to use can be considered valid in absence of convective movements.

Fourier's law of heat conduction

$$\frac{\partial^2 T}{\partial x^2} = \frac{\rho c}{\lambda} \frac{\partial T}{\partial t} \quad (4.5)$$

$$\alpha = \frac{\lambda}{\rho c} \quad (4.6)$$

$$\frac{\partial^2 T}{\partial x^2} = \frac{1}{\alpha} \frac{\partial T}{\partial t} \quad (4.7)$$

This is a second order PDE. We need to change it in an ODE in order to find an analytical solution. We introduce a new variable and make temperature dimensionless using  $\Theta$ .

$$\xi = \frac{x}{\sqrt{\alpha t}} \quad (4.8)$$

$$\Delta T = T_0 - T_w \quad (4.9)$$

$$\frac{\partial T}{\partial t} = \Delta T \frac{\partial \Theta}{\partial t} = \Delta T \frac{\partial \xi}{\partial t} \frac{\partial \Theta}{\partial \xi} = \Delta T \left( -\frac{x}{2t\sqrt{\alpha t}} \right) \frac{\partial \Theta}{\partial \xi} \quad (4.10)$$

We do the same thing with second derivative

$$\frac{\partial T}{\partial x} = \Delta T \frac{\partial \xi}{\partial x} \frac{\partial \Theta}{\partial \xi} = \frac{\Delta T}{\sqrt{\alpha t}} \frac{\partial \Theta}{\partial \xi} \quad (4.11)$$

$$\frac{\partial^2 T}{\partial x^2} = \frac{\partial}{\partial x} \left( \frac{\Delta T}{\sqrt{\alpha t}} \frac{\partial \Theta}{\partial \xi} \right) = \frac{\Delta T}{\alpha t} \frac{\partial^2 \Theta}{\partial \xi^2} \quad (4.12)$$

By substituting the first and the last of these derivatives in heat conduction equation, we get

$$\frac{d^2 \Theta}{d\xi^2} = -\frac{\xi}{2} \frac{d\Theta}{d\xi} \quad (4.13)$$

Initial condition for previous equation is

$$T(t = 0) = T_i \quad (4.14)$$

$$\Theta(\xi \rightarrow \infty) = 1 \quad (4.15)$$

and the one known boundary condition is

$$T(x = 0) = T_w \quad (4.16)$$

$$\Theta(\xi = 0) = 0 \quad (4.17)$$

If we call  $d\Theta/d\xi \equiv \chi$  we obtain an ODE

$$\frac{d\chi}{d\xi} = -\frac{\xi}{2}\chi \quad (4.18)$$

which can be integrated once to get

$$\chi \equiv \frac{d\Theta}{d\xi} = C_1 e^{-\xi^2/4} \quad (4.19)$$

and we integrate this a second time to get

$$\Theta(\xi) = C_1 \int_0^\xi e^{-\xi^2/4} d\xi + \Theta(0) \quad (4.20)$$

The b.c. is now satisfied and we need only substitute  $\Theta(\xi)$  in the i.c. to solve for  $C_1$ :

$$1 = C_1 \int_0^\xi e^{-\xi^2/4} d\xi \quad (4.21)$$

The definite integral is given by integral tables as  $\sqrt{\pi}$ , so

$$C_1 = \frac{1}{\sqrt{\pi}} \quad (4.22)$$

Therefore solution to the problem of conduction in a semi-infinite region, subject to a b.c. of the first kind is

$$\Theta = \frac{1}{\sqrt{\pi}} \int_0^\xi e^{-\xi^2/4} d\xi = \frac{2}{\sqrt{\pi}} \int_0^{\xi/2} e^{-s^2} ds \equiv erf(\xi/2) \quad (4.23)$$

*erf* is called *error function*. We can calculate  $\xi/2 =$  for  $x$  during time. Then we can find  $\Theta$  and the relative value of temperature.

In our tests  $T_0$  is the initial temperature of water that we assume be the same as the ambience temperature.  $T_w$  is the temperature of the bottom of the cylinder that we assume to be constant because of thermostatic bath.

We used this method for evaluate time needed to cool substantially water in the mixer. In the graphs x-axis is the height of water in the cylinder.

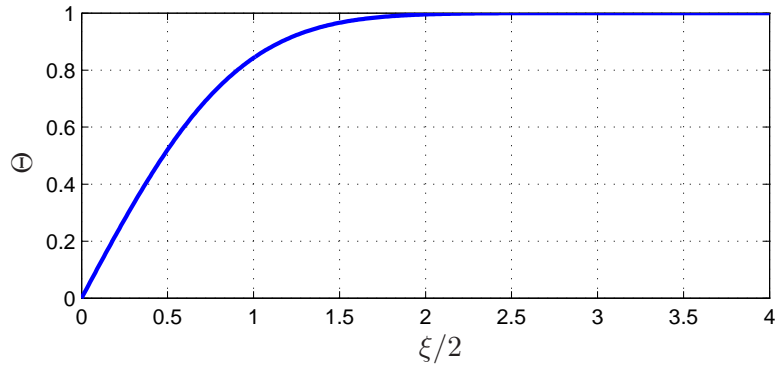
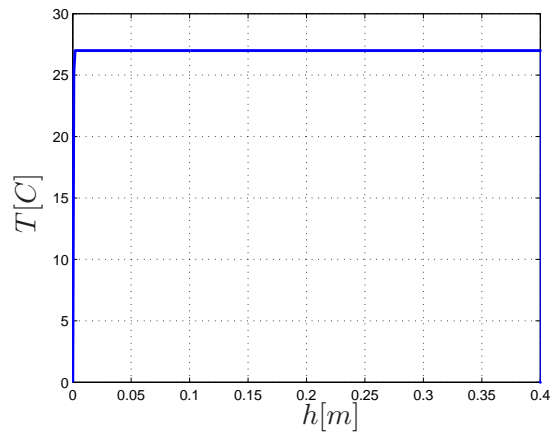


Figure 4.4: Error function

Figure 4.5: Theoretical temperature distribution in the cylinder at  $t=0$

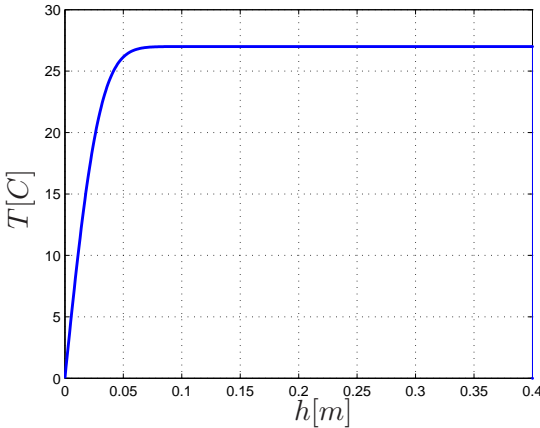


Figure 4.6: Theoretical temperature distribution in the cylinder at  $t=1800s$

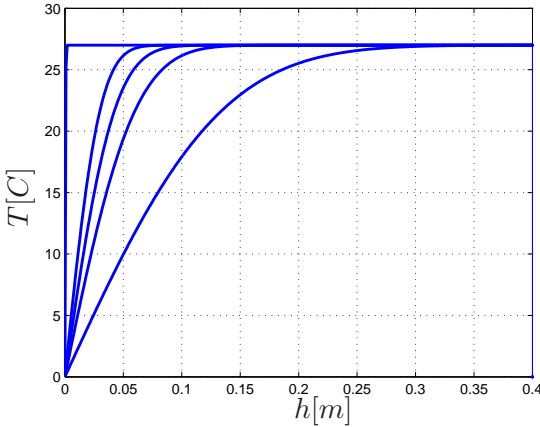


Figure 4.7: Theoretical temperature at  $t=[0,1800,3600,7200]s$



## Chapter 5

# Experimental Setup

### 5.1 Design choices

Designing the experimental setup was the first step of this research work. We decided to make tests using measures of temperature.

The first idea was to cool the bottom of the mixer, but after the first tests we decided to improve the setup including a heating system in the top layer. This solution allowed us to heat or cool the water without convective movements. We placed 27 thermocouples to measure the temperature along the entire height of the cylinder. We used as many thermocouples as we could acquire because we want to have the more accurate data as possible. We measured the average temperature of the water inside the mixer and we calculated the amount of energy given or subtracted from the system. In every test we exchange with the water the same amount of energy. The thermocouples allowed us to identify the mixing time with Matlab.

We used an external power supply to power the motor to avoid problems of electric instability. We put a current sensor between the motor and the power supply and we calculated the electric power consumption using the acquired data of the current and the voltage.

The main aim of this work was to test the mixer using the rotational velocity of the mixer as reference. For this reason we used a motor equipped with encoder for the highest accuracy possible.

The experimental setup changed during the preliminary tests. We improved it adding some useful elements: a tap to empty the cylinder, a hole in the cap to fill it and a covering of insulating material.

## 5.2 3D model

We used SolidWorks[2] to design the mixer. This program allowed us to be very precise in designing each part and it made faster the creating phase.



Figure 5.1: 3D model of the mixer

The main dimensions of the mixer are these:

internal cylinder diameter	14cm
external cylinder diameter	15cm
cylinder height	40cm
shaft diameter	6mm

Initially we designed an external support for the motor but we found that the setup was heavy enough to avoid excessive vibrations therefore we mounted the motor on top of the mixer.

Main components of the mixer:

- a slinky spring
- a plexiglass cylinder
- a cap of PVC
- an aluminum shaft
- a rigid joint



- an aluminum circular bottom
- two supports for the slinky
- a column of corial for the thermocouples
- a square aluminum base
- a base of corial for the heat exchanger
- some o'ring

### 5.3 Configurations of the mixer

We tested four different configurations of the mixer:

- free slinky+ that moves counter-clockwise
- free slinky- that moves clockwise
- fixed slinky that moves counter-clockwise
- impeller that moves counter-clockwise

The slinky used has a diameter of  $3\text{cm}$  and 70 coils. We fixed one terminal at  $85\text{mm}$  from the bottom of the mixer then we twisted the slinky 2 times and fixed the other terminal at  $29\text{cm}$  from the bottom. We used a  $120\text{mm}$  diameter impeller fixed it at  $10\text{cm}$  from the bottom of the mixer.

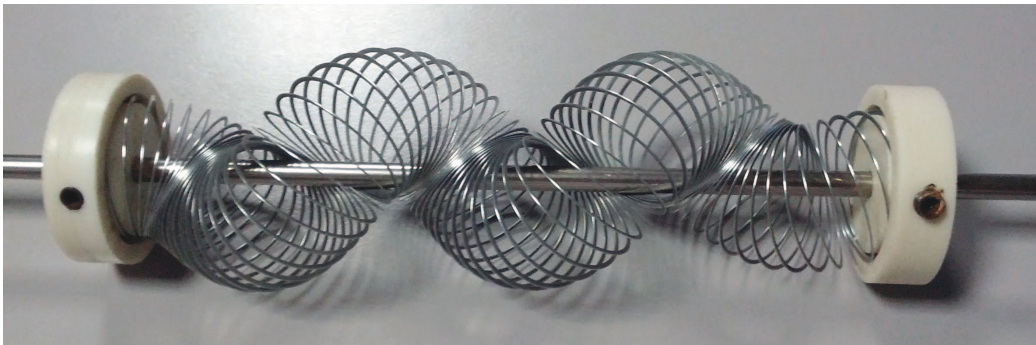


Figure 5.2: Slinky spring mounted on the shaft

## 5.4 Power supply

**Agilent E3631A** The Agilent E3631A (fig. 5.3) is a high performance 80 watt-triple output programmable DC power supply. In our tests we usually used +25V output regulated by control knob. We could change the voltage very precisely with a minimum step of 0.01V. Using "Output On/Off" button it was possible to set up the value of the output voltage and to turn the output on when needed.



Figure 5.3: Programmable DC power supply Agilent E3631A

**Secondary power supply** We used a non controlled secondary DC power supply for the heating system. The output voltage of this power supply is 13V. Using a resistor of  $6\Omega$  we created a 20W heating system.

## 5.5 Heating and cooling system

**Cooling system** Since the bottom of the mixer is an heat exchanger we used a thermostatic bath to cool it. Water enters in the base and exchanges heat with the mixer aluminum bottom and then returns to the thermostatic bath.

**Heating system** We created a circular resistor of  $6\Omega$  and used some non-conductive elements as a supporting structure. We attached it to a long screw with two nuts. This screw passes through the cap and we could change its height with another nut.

## 5.6 Motor

During the preliminary tests we tried different motors. After several tests we decided to use a Pololu Metal Gearmotor 37Dx52L mm (fig. 5.6).

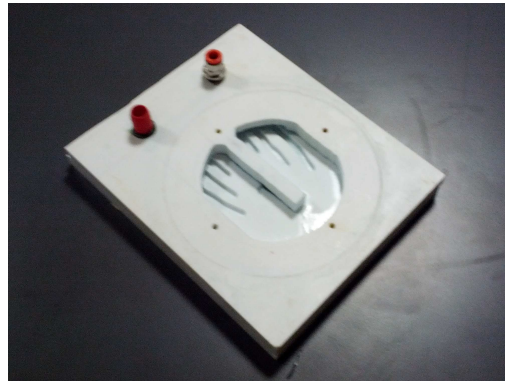


Figure 5.4: Particular of the heat exchanger under the mixer

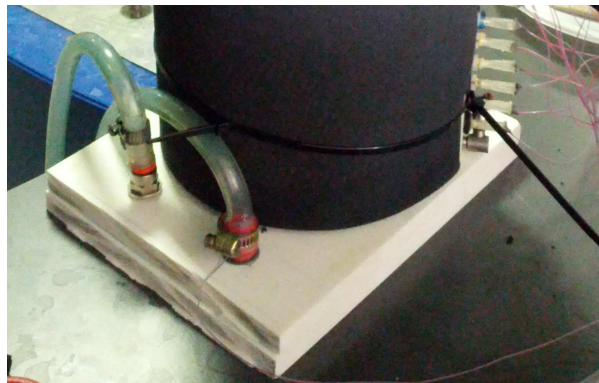


Figure 5.5: View of the heat exchanger under the mixer



Figure 5.6: Metal Gearmotor 37Dx52L mm

Gear Ratio	19:1
Speed 12V	500rpm
Stall Torque 12V	84 oz-in
Stall Current 12V	5A

Table 5.1: Pololu motor characteristics

This motor has a very linear characteristic curve with no irregularities especially at the low velocities.

## 5.7 Sensors

### 5.7.1 Thermocouples

We built our thermocouple using a thermocouple wire<sup>1</sup> from TERSID.S.r.l. and medical tip-less needles. We fixed the wire using industrial glue. Then we put these sensors in drilled screws that were inserted in the holes of the cylinder.

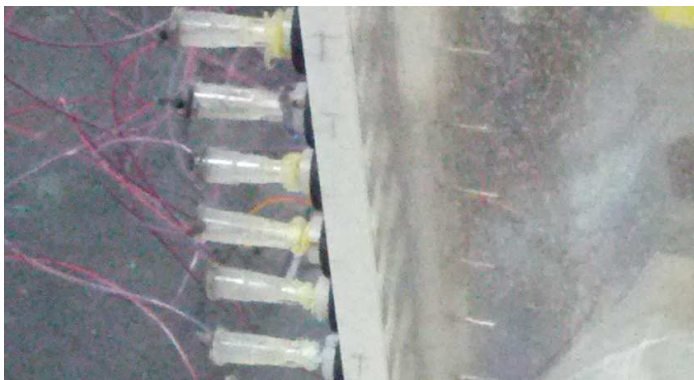


Figure 5.7: View of thermocouples

We created 27 thermocouples with needles and 2 without them. We used these two to measure ambient temperature and bottom heat exchanger temperature. We linked all the thermocouples to the NI 9213 to acquire data.

### 5.7.2 Current sensor

We measured current using a ACS712 that has a  $V_{cc}$  of 5V and we linked it to the output voltage of the NI6009. We mounted it on the wire that links the motor to the power supply. The output is a voltage but we used its data-sheet to calculate the current.

---

<sup>1</sup>TEX-36-TT

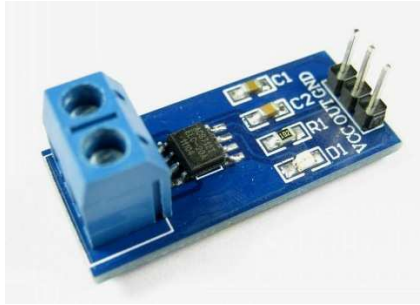
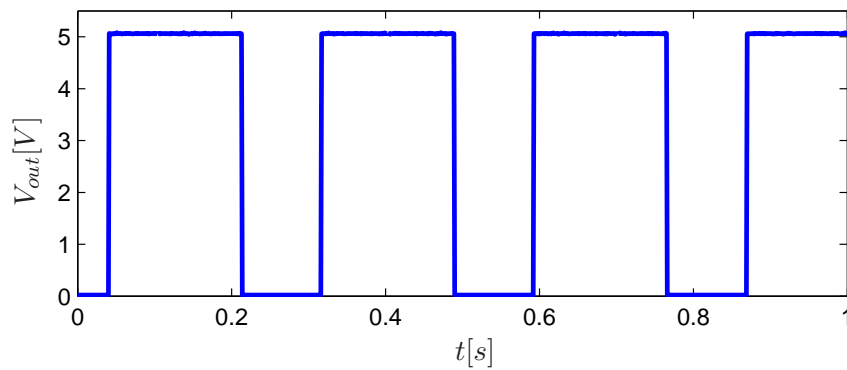


Figure 5.8: Current sensor ACS712

### 5.7.3 Encoder

It needs  $5V$  as  $V_{cc}$  and so we linked it to the NI6009 too. A magnet is attached to the shaft of the motor. The voltage output becomes null every time the magnet passes near the sensible surface of the sensor. In every other situations the output is  $5V$ .

The output of the Encoder is a square wave (fig. 5.9). By knowing time between two ridges we could measure the *rps*.

Figure 5.9: Example of encoder square wave output [ $3.65rps$ ]

## 5.8 Acquisition system

In each test we acquired this data:

- temperature of each thermocouples
- output voltage of the encoder
- motor current

### 5.8.1 LabVIEW

NI LabVIEW is a software for the design of systems that uses icons, terminals and connections rather than text, so you can program the way you think. LabVIEW includes tools based on advanced programming features for the development of control applications, measurement and analysis with professional user interfaces. We used it for acquiring data from two NI9213 and from NI9205. We created a custom interface which allowed us to see the value of all thermocouples and encoder output (fig. 5.10).

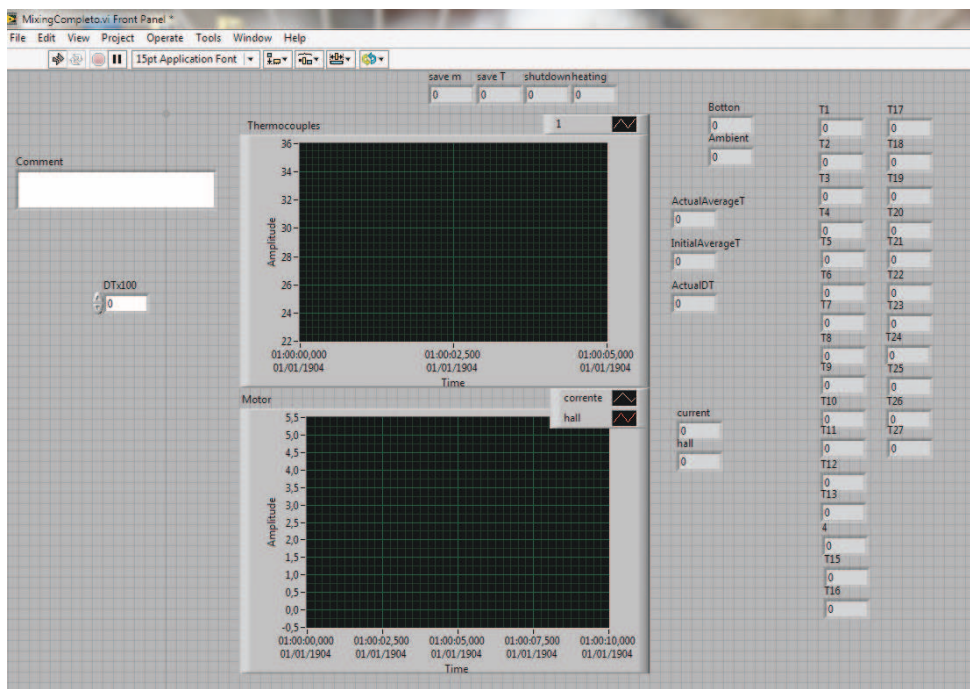


Figure 5.10: Screenshot of LabVIEW virtual instrument

When a test starts the system saves the value of the average temperature and every time it calculates its variation. You can choose a value of average temperature maximum increase. When average temperature reaches this value

LabVIEW make an alert sound. During all the test LabVIEW saves temperatures data. The motor data are saved only at the initial time and when the heating phase is over. The thermocouples data are acquired at a rate of  $3Hz$  while the motor data are acquired at  $1KHz$  [5].

### 5.8.2 NI USB-6009

NI USB-6009 provides basic data acquisition functionality for applications, data logging, portable measurements and laboratory experiments. These cards have an accessible cost to students and offer adequate performance for more sophisticated measurement applications.



Figure 5.11: Low-Cost Multifunction DAQ NI USB-6009

We used it to power encoder and current sensor.

### 5.8.3 NI9213 and NI9205

**The NI9213** is a high-density thermocouple module for NI C Series carriers designed for higher-channel-count systems. With this module, you can add thermocouples to mixed-signal test systems without taking up too many slots. Built-in cold-junction compensation is the main feature of this device.

We used two of this device to acquire all the temperatures of the thermocouples.

**The NI9205** is a C Series module, for use with NI CompactDAQ and CompactRIO chassis. The NI9205 features 32 single-ended or 16 differential analog inputs, 16-bit resolution, and a maximum sampling rate of  $250 kS/s$ .

We used this device to acquire current sensor and encoder outputs.



Figure 5.12: Thermocouple Input Module NI9213



Figure 5.13: Voltage Input Module NI9205



## 5.9 Matlab

We used Matlab to post-process the acquired data. We divided the post-process in two main parts: one for the temperature data and one for the motor data.

### 5.9.1 Post-process of temperature data

These are the functions created for the temperature data:

- **loadifle.m** it opens the data file and saves the time in a vector and the temperatures of all the thermocouples in a matrix
- **smooth.m** it smooths the data by applying a moving average of  $N$  points
- **mixing.m** it calculates the derivative of the temperatures to find where the mixing is. It finds the maximum of the derivative and then moves forward to find where the STD became littler than 0.0005 that mean an homogeneity of 97.75%.
- **calibration.m** it calculates the difference between the final average temperature of each thermocouple and the total average temperature
- **energy.m** it calculates the average temperature
- **graph.m** it makes graph of the total test (fig. 5.14)
- **graphmixing.m** it makes graph of the interval of mixing (fig. 5.15)

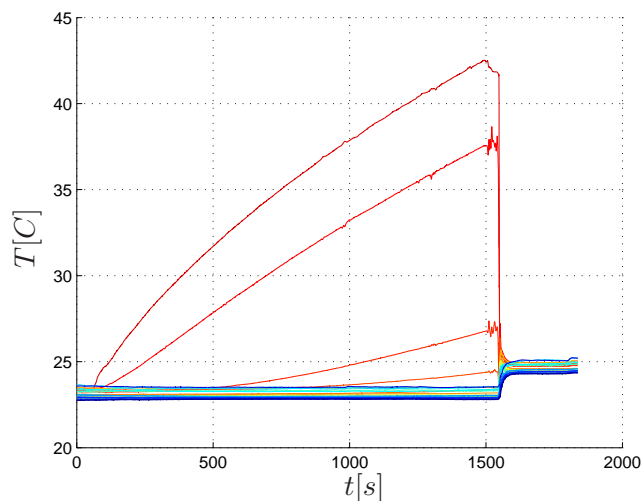


Figure 5.14: Example of total graph of a test [3.65rps]

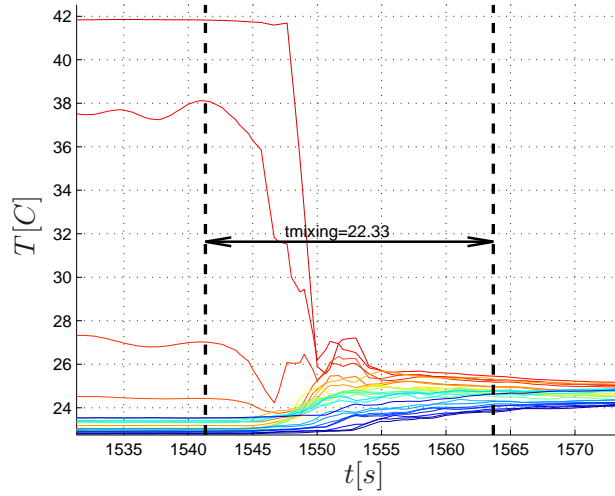


Figure 5.15: Example of mixing graph of a test [3.65rps]

### 5.9.2 Post-process of motor data

The motor data were saved in two different files: one for the encoder and one for the current sensor.

We took the data in different times. We took the encoder data during the main tests. The current data were taken after them. Initially we measured current by acquiring voltage of a  $1\Omega$  resistor in series with the motor but we discovered that measures were wrong. After all tests we calibrated the motor for every configuration and at every velocity (fig. 5.18).

We used the original current data to identify the start of the mixing in each test and to correct the value identified by studying the *STD*. In figure 5.17 you can see that the current is null until 1596s. After this value it becomes bigger because LabVIEW is acquiring the current but the power supply is off so there is only electrical noise. At 1635s we turned on the motor.

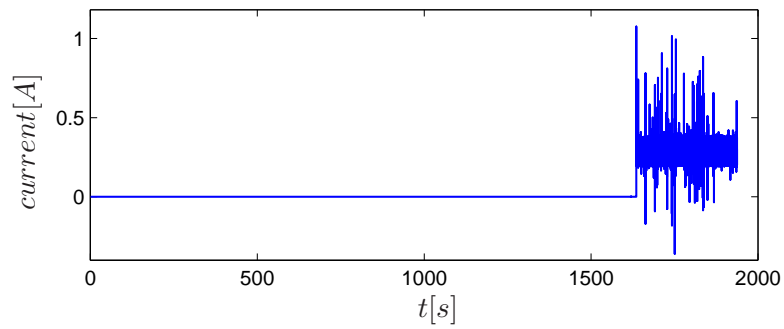


Figure 5.16: Example of original current data of a test [3.65rps]

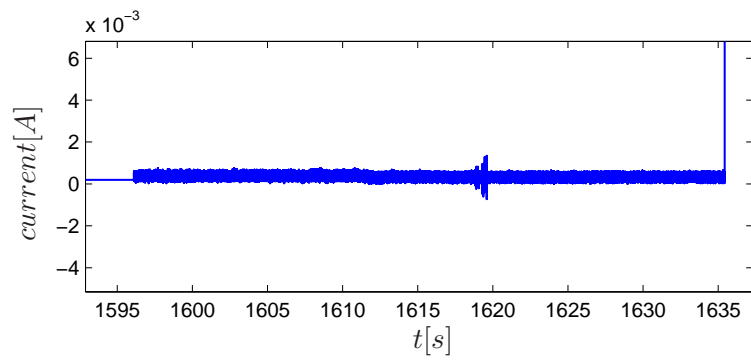


Figure 5.17: Example of locating the beginning of the mixing [3.65rps]

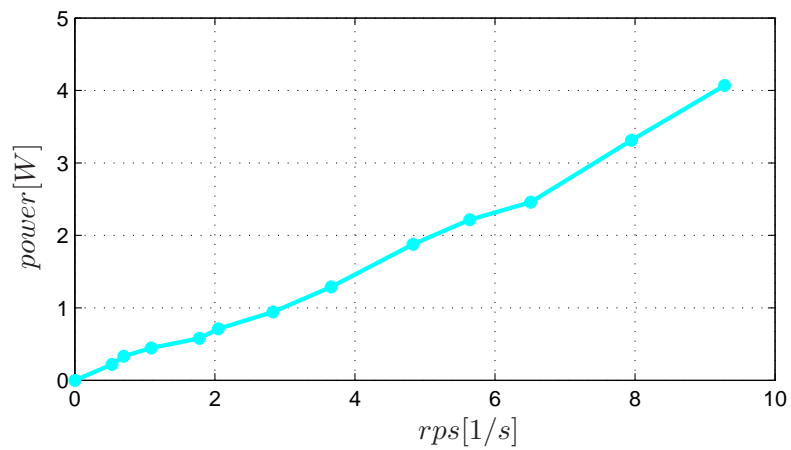


Figure 5.18: Example of power on rps graph

## 5.10 Experimental Procedure

This is the experimental procedure of each test<sup>2</sup>:

1. turn on the motor and set the required speed
2. disconnect the motor
3. wait until the water stops
4. start the program data acquisition on LabVIEW
5. turn on the resistor
6. wait until the average temperature increases of 1.5° C
7. turn off the resistor
8. remove the resistor from water and block it
9. reconnect the motor
10. wait until the temperatures becomes stable
11. post-process acquired data.

---

<sup>2</sup>Before every set of test we filled the mixer with water until the height of the first thermocouple. At the end of daily tests we emptied it.

## 5.11 Diagram of the experimental setup

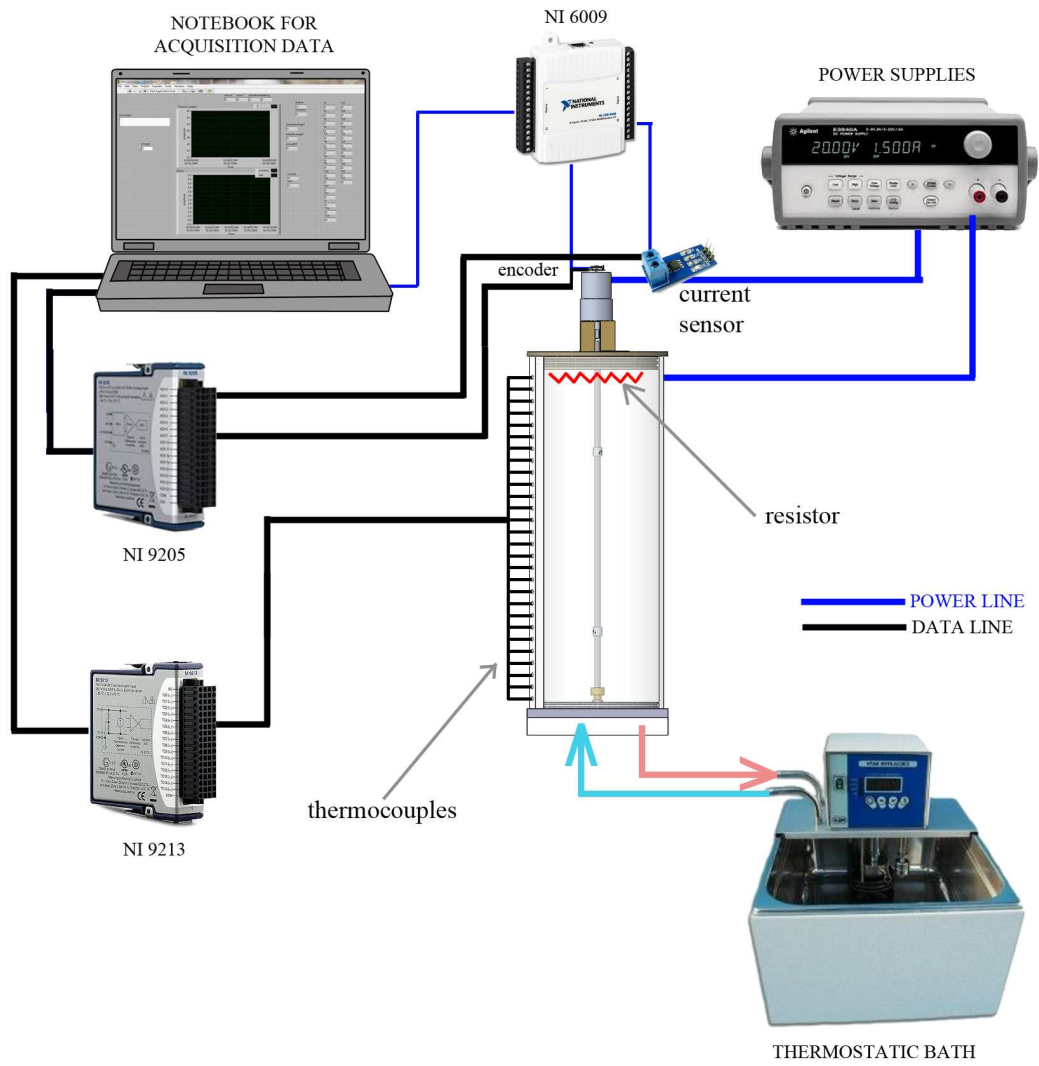


Figure 5.19: Diagram of the experimental setup



# Chapter 6

## Validation

### 6.1 Test of the thermocouples

**Impermeability test** We inserted every thermocouple produced in a little pipe linked to a syringe full of water to test their impermeability. The resulting water losses are minimal.

**Calibration tests** We tested all of the thermocouples using a thermostatic bath with melting ice and we recorded a maximum temperature difference of  $0.1^{\circ}C$ . We also analysed the difference between the average temperature of each thermocouple and the total average temperature at the end of every test. We choose to not modify the calibration curve by inserting an offset for each thermocouple.

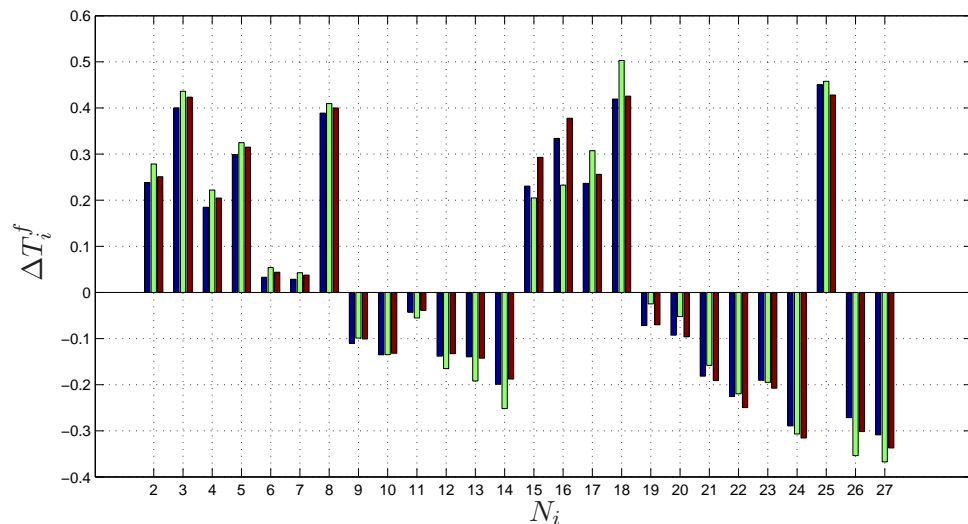


Figure 6.1:  $\Delta T_i^f$  for three tests at  $3.65rps$

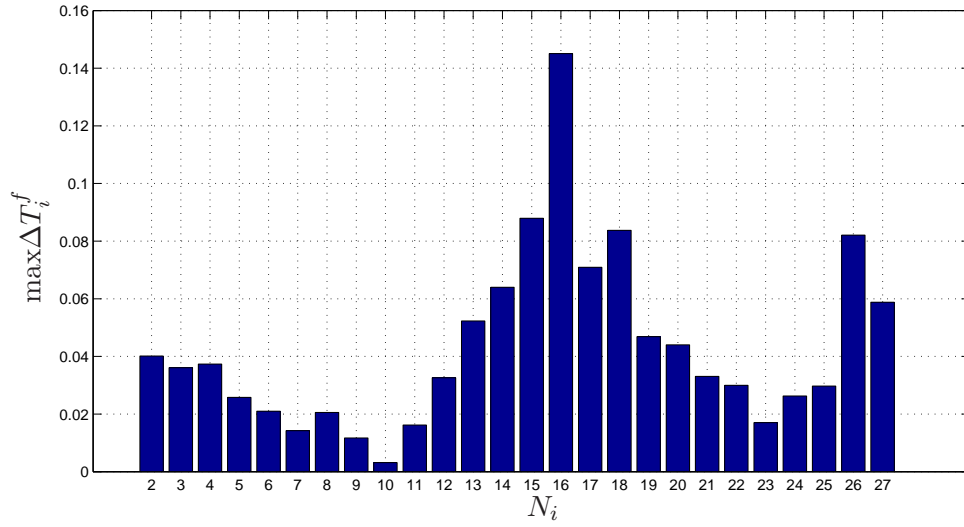


Figure 6.2: Maximum value of variation  $\Delta T_i^f$  for three tests at  $3.65 rps$

In figure 6.1 we plot the values of  $\Delta T_i^f$ . The data of this graph are taken from three tests that we did in succession at the same velocity ( $3.65 rps$ ) with slinky+. In the figure 6.2 we calculated the maximum variation of  $\Delta T^f$  for each thermocouple.

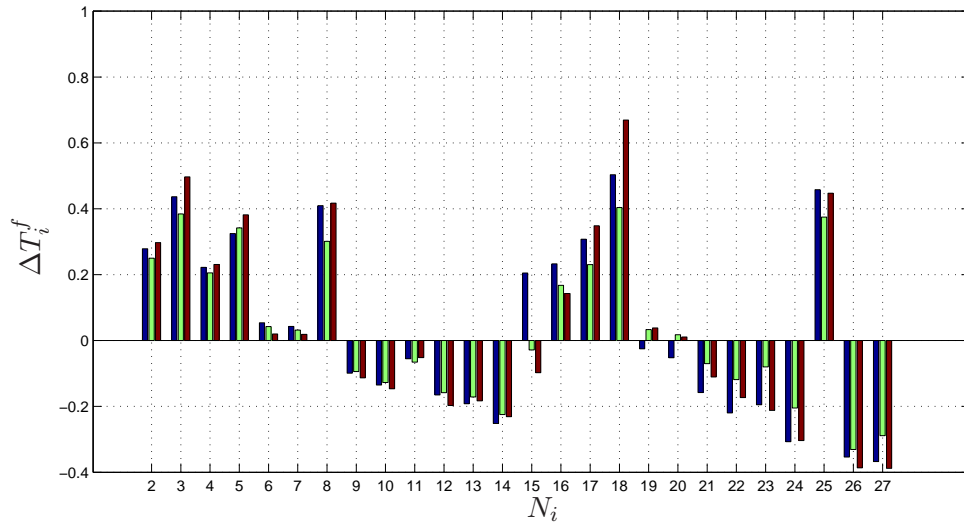


Figure 6.3:  $\Delta T_i^f$  for three tests at  $3.65 rps$  with different configurations



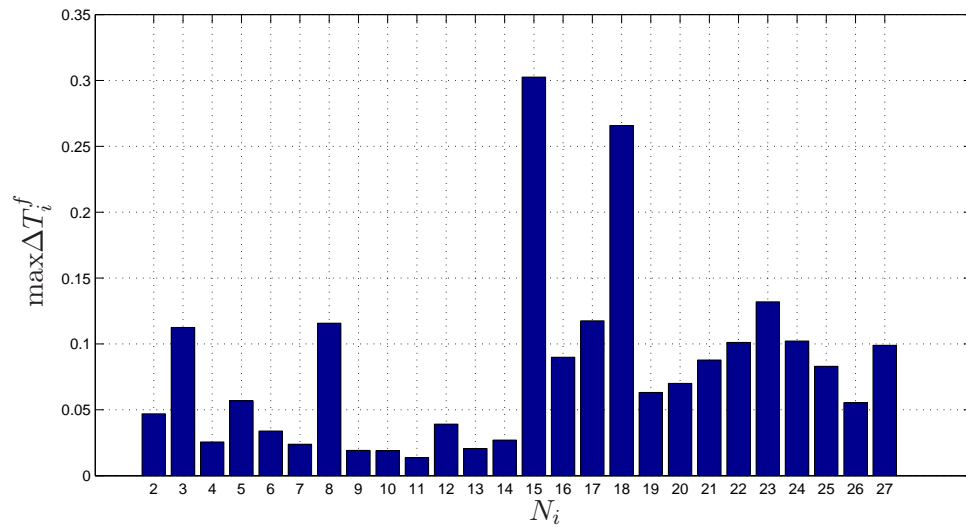


Figure 6.4: Maximum value of variation  $\Delta T_i^f$  for three tests at  $3.65 rps$  with different configurations

In figures 6.3 and 6.4 we compared three tests with three different configurations of the slinky at the same velocity ( $3.65 rps$ ).

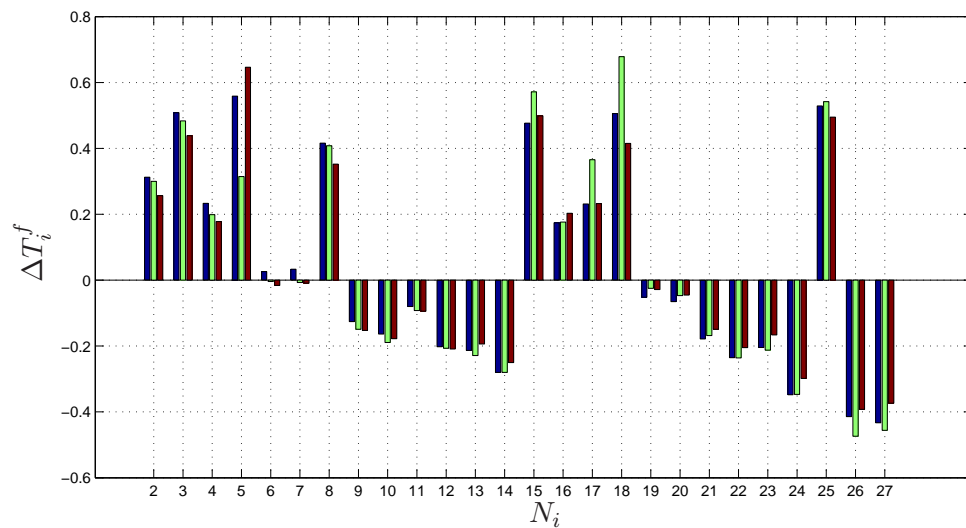


Figure 6.5:  $\Delta T_i^f$  for three tests at  $[0.53, 1.79, 7.94] rps$

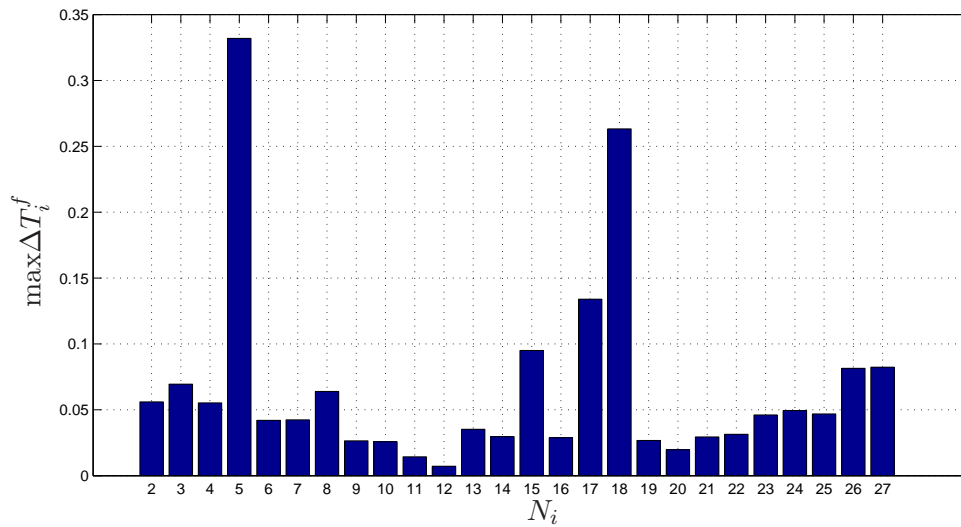


Figure 6.6: Maximum value of variation  $\Delta T_i^f$  for three tests at  $[0.53, 1.79, 7.94]$  rps

In figures 6.5 and 6.6 we compared three tests<sup>1</sup> with three different velocities<sup>2</sup> made in three different days.

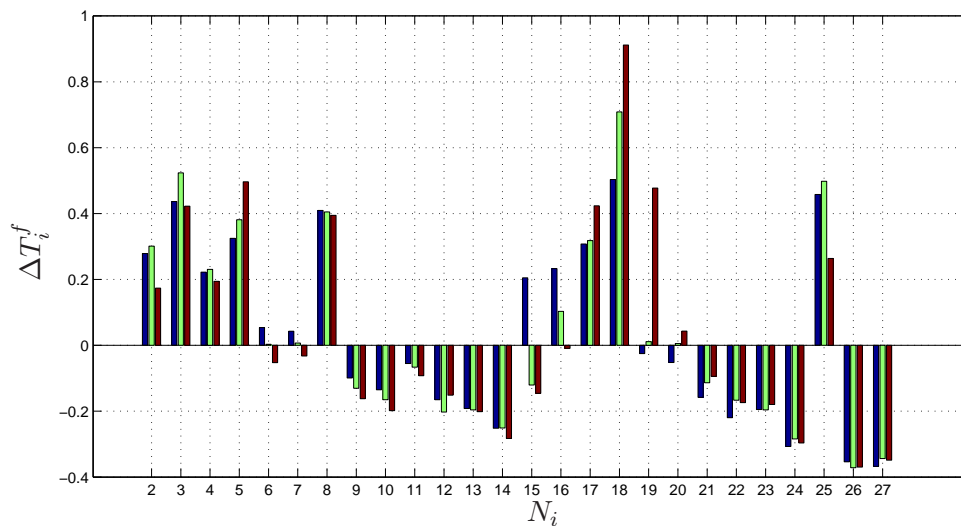


Figure 6.7:  $\Delta T_i^f$  for three tests at different velocities with different configurations

<sup>1</sup>slinky+

<sup>2</sup> $[0.53, 1.79, 7.94]$  rps

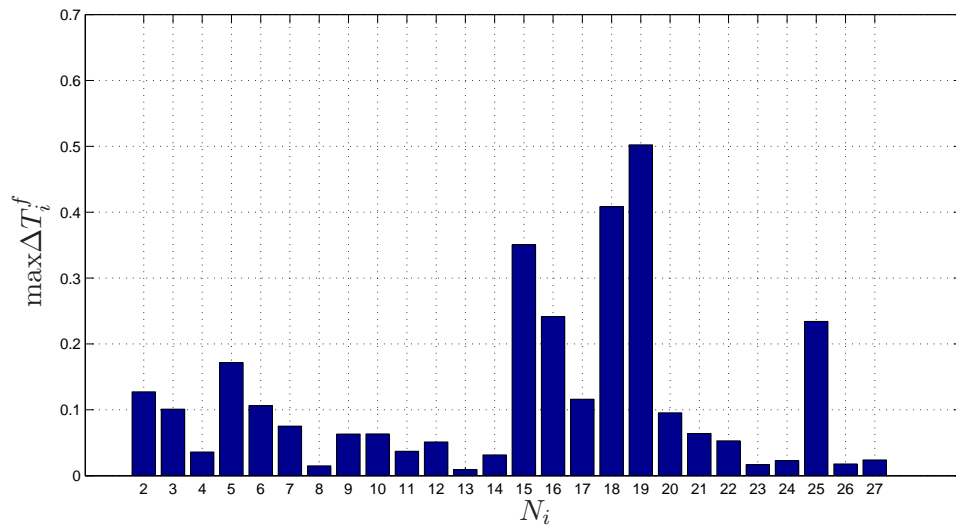


Figure 6.8: Maximum value of variation  $\Delta T_i^f$  for three tests at different velocities with different configurations

Finally we compared three different configurations<sup>3</sup> at three different velocities [3.65,9.43,2.95]*rps* (fig. 6.7 and 6.8).

We proved that the thermocouples do not change their behaviour. In fact, as can be see from the graphs, they maintain the same distribution of  $\Delta T_f^i$ . We recorded the main variations when we compared tests of different configurations.

Finally we assumed homogeneous temperature at the start and the end and of each test (for example fig. 6.9 and 6.10)<sup>4</sup>. We found little variations so we can also prove that the thermocouples don't change their characteristics during a test.

<sup>3</sup>free slinky+,fixed slinky and impeller all moving counter-clockwise

<sup>4</sup>slinky+ at 2.05*rps*

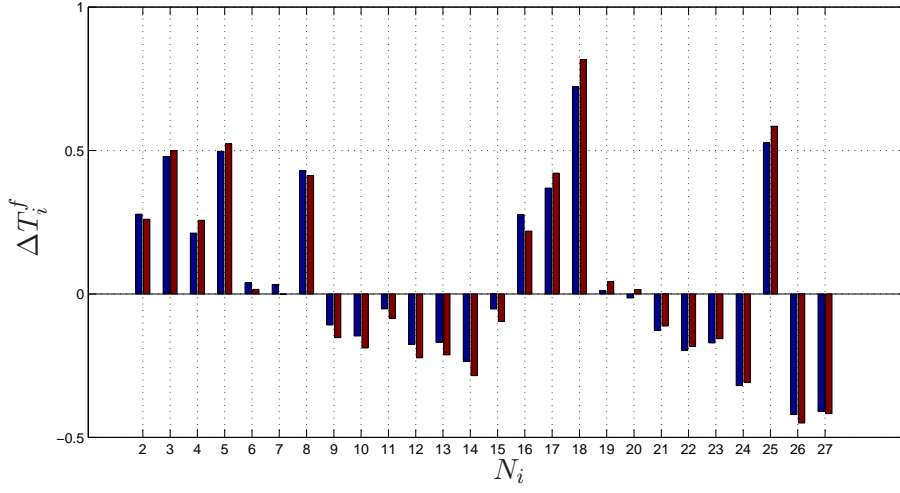


Figure 6.9:  $\Delta T_i^{tot}$  between  $T_a^i$  and  $T_a^f$

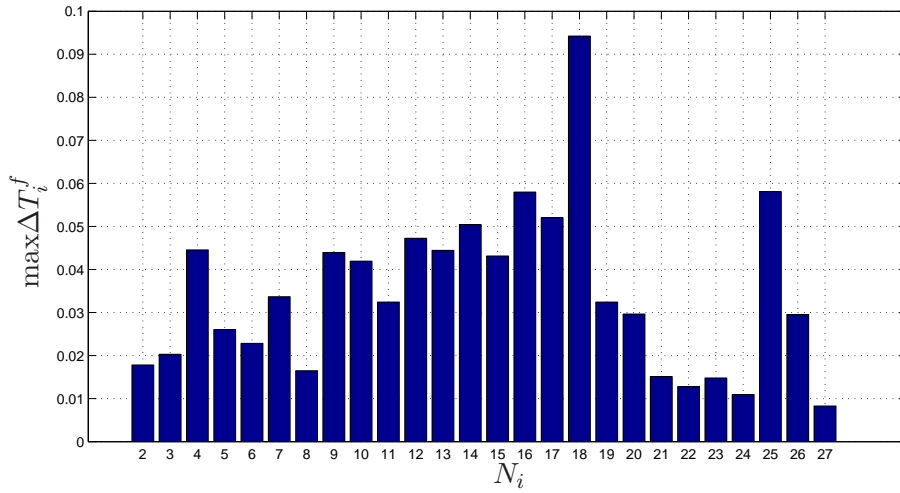


Figure 6.10: Maximum value of variation  $\Delta T_i^{tot}$  between  $T_a^i$  and  $T_a^f$

## 6.2 Cooling test

Initially we decided to make tests using the thermostatic bath to cool down the bottom of the cylinder. The main idea was to let the water stratify and then turn on the mixer. We filled the cylinder and then we set the bath at a temperature of  $5^{\circ}\text{C}$ . We left the setup work through the night<sup>5</sup>. The day after the water was totally stratified (fig. 6.11). The found data were consistent with the theory of heat transfer in semi-infinite plane (fig. 6.12)<sup>6</sup>.

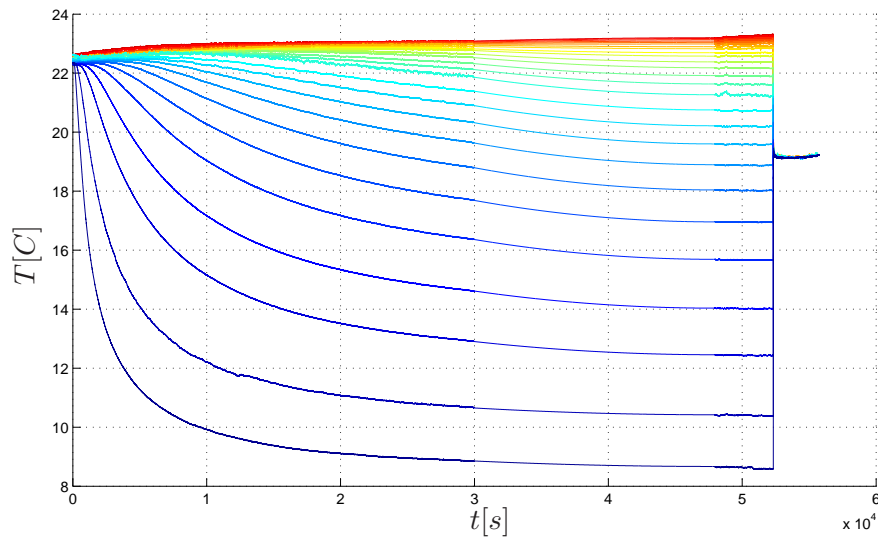


Figure 6.11: Stratification of the water with the cooling system

We tried to understand how much time is necessary to have a substantial change of temperature in the cylinder. We have estimated that it takes about three hours to get a sufficient stratification for a test.

The main problem of this system is that we had limitations with cooling:  $\Delta T$  between  $T_a^i$  and the bottom temperature had a lower limit.

## 6.3 Heating test

We decided to improve the setup adding a heating system in the top part of the mixer. First we tried to understand if heating was better than the cooling. We made some preliminary tests with the resistor that we turned on for 30 minutes (fig. 6.13).

<sup>5</sup>we extrapolated some data because the pc turned off

<sup>6</sup>we used similar boundary and initial conditions

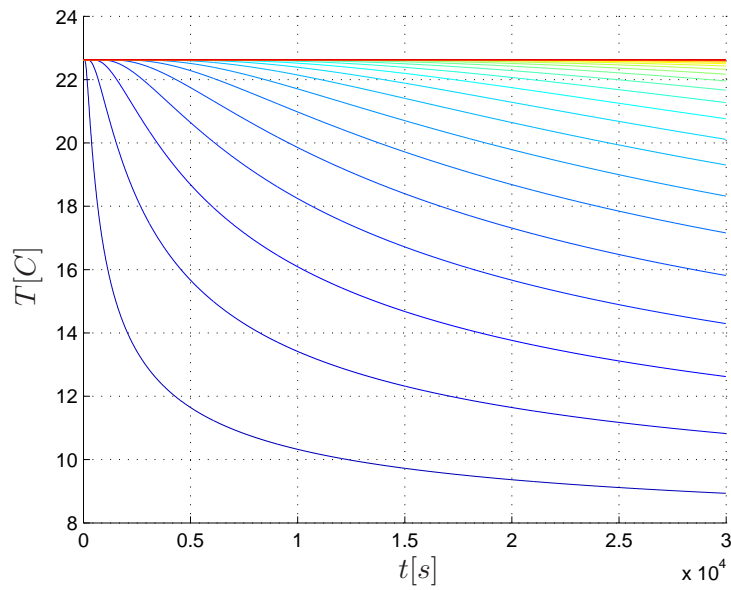


Figure 6.12: Stratification using the theory of heat transfer in semi-infinite plane

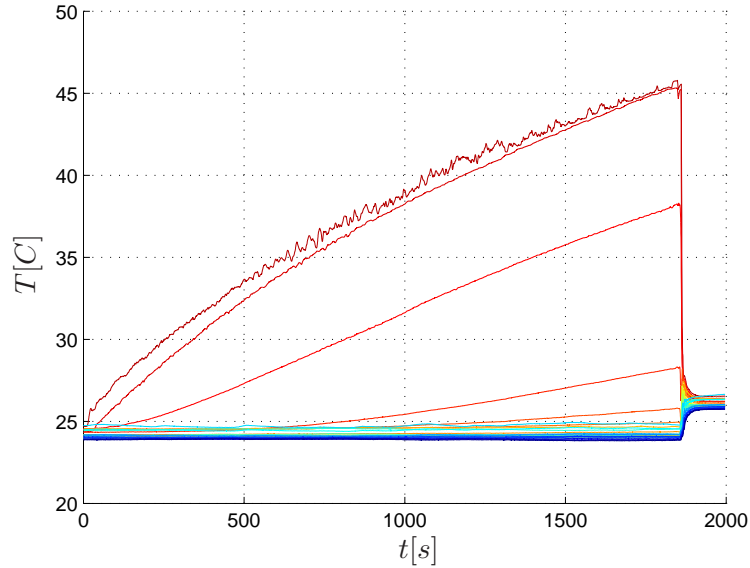


Figure 6.13: Stratification of the water with the heating system

The convective movements generated by the resistor distribute heat to all the top layer.

We had a significant variation of the temperature inside the mixer, probably because we were able to reach a greater  $\Delta T$  between water and heating system than  $\Delta T$  of the cooling system. In fact after 30 minutes the highest thermocouple reached  $45^{\circ}\text{C}$  that means an increase of  $20^{\circ}\text{C}$ . In the cooling test after 30 minutes the greatest variation was about  $7^{\circ}\text{C}$ .

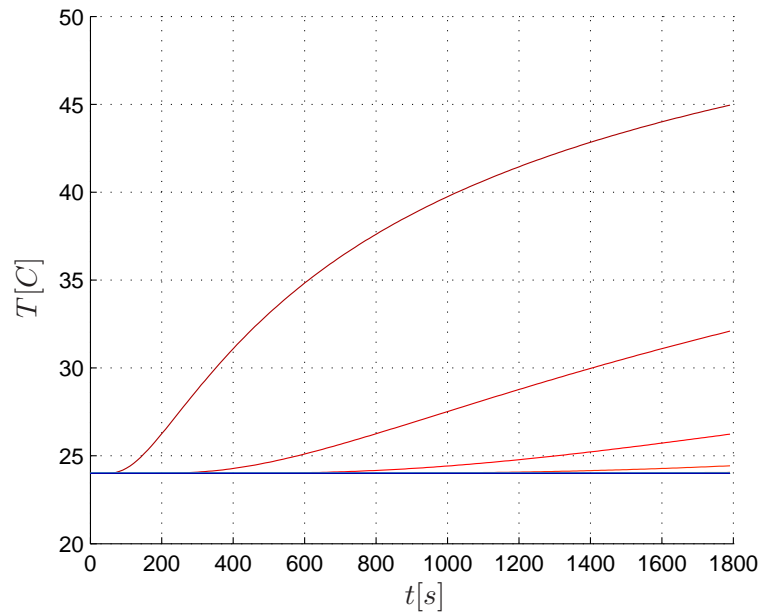


Figure 6.14: Stratification of the water using the theory of heat transfer in semi-infinite plane with hot wall

We used the theory of heat transfer in semi-infinite plane also with the heating case (fig. 6.14). We didn't know the value of the hot wall so we used an iterative code to find it. In this test it was about  $64^{\circ}\text{C}$ .

## 6.4 Mixing time procedure test

You have to choose a grade of homogeneity to measure the mixing time. Generally if you have a probe you can normalized its output.

$$C'_i = \frac{C_i - C_0}{C_\infty - C_0} \quad (6.1)$$

Where  $C_i$  is the value of the probe output at time  $i$ ,  $C_0$  is the initial value and  $C_\infty$  is the final stable value. We knew the start time of the mixing by motor data. We tried to identify the mixing time using this definition. We measured different times for tests (a,b) with equal conditions (fig. 6.15 and 6.16).

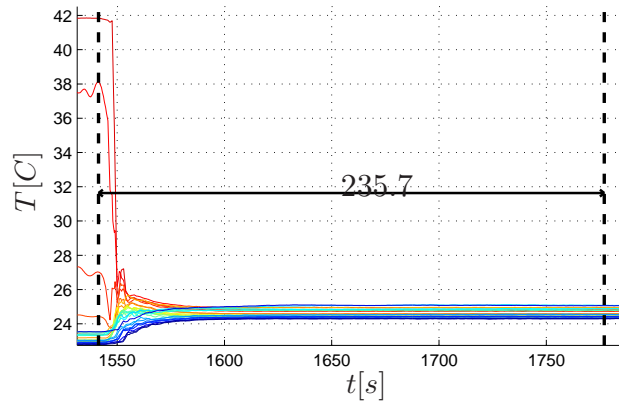


Figure 6.15: Mixing time (a) using classical definition

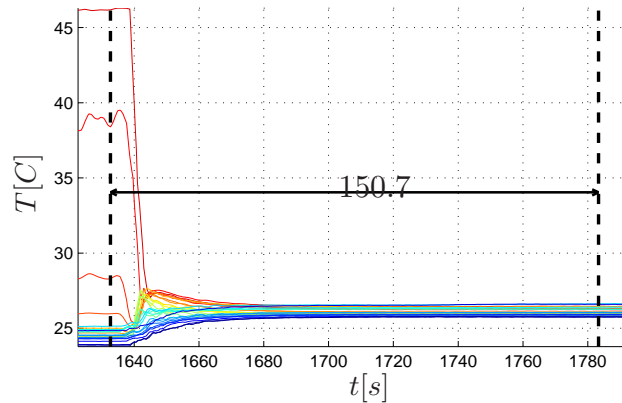


Figure 6.16: Mixing time (b) using classical definition

The problem was that in our test  $C_\infty$  was not a stable value because of heat exchange with ambience. The final value of temperatures depends on time of



the test. We decided to change the method to identify mixing time. We started studying the absolute value of the derivatives of the temperatures. We calculated them with finite difference (fig. 6.17).

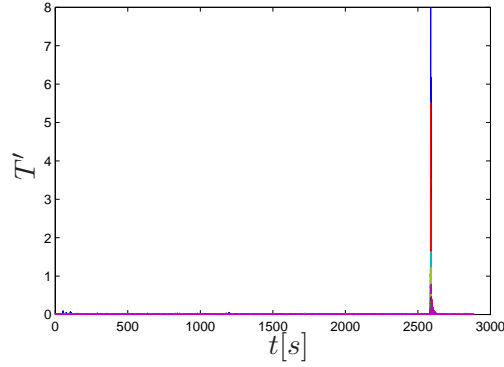
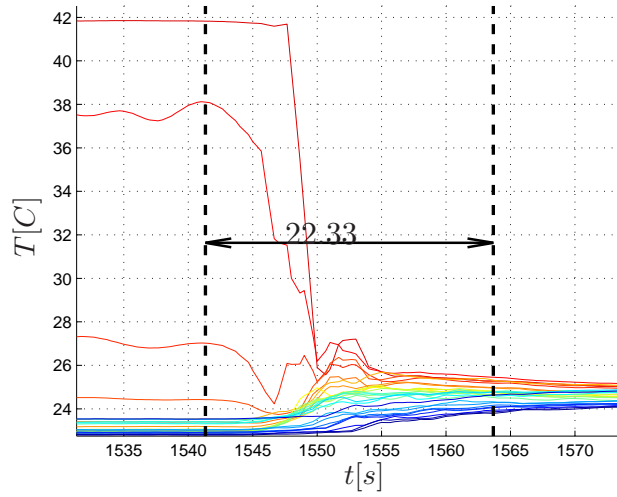
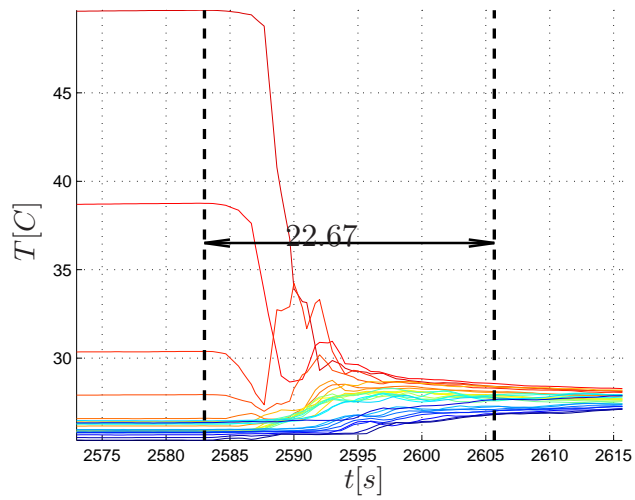


Figure 6.17: Absolute value of the derivative of the temperatures

The derivatives were always very low. In the mixing area they varied remarkably. Then they became low again. In each test we searched for the maximum value of the derivatives and the relative instant. Then we went forward in time until the maximum *STD* became less than 0.0005. In this conditions the temperature could be considered homogeneous. Using *STD* method we found the same value of mixing time (fig. 6.18 and 6.19).

We defined *STD* as:

$$\sigma_i(t) = \left( \frac{T_i(t) - (T_i^f - T_a^f)}{T_a(t)} - 1 \right)^2 \quad (6.2)$$

Figure 6.18: Mixing time (a) using *STD* methodFigure 6.19: Mixing time (b) using *STD* method

## 6.5 Test of the experimental procedure

In any mixing test it is necessary to impose some quantity that has to be mixed. We tried different procedures to have the same quantity of energy for each test. Initially we turned on the resistor for 30 minutes, we mixed water and then we started another test. We supposed that using the same resistor for the same time gave the same energy to water. In this way we measured different mixing times (fig. 6.20 and 6.21).

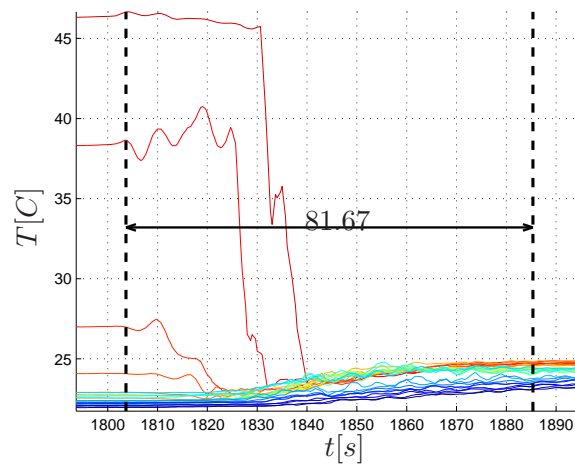


Figure 6.20: Example of a test of 30 minutes of heating

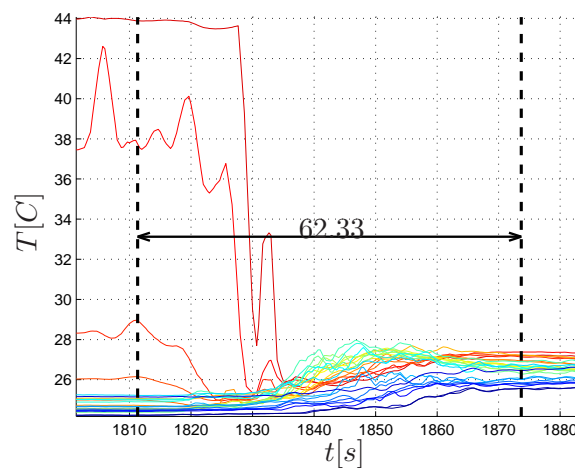


Figure 6.21: Another example of a test of 30 minutes of heating

The problem is that with a high initial average temperature the mixing time decreases because the resistor gives less energy to the system. We can calculate the energy given to the system in this way:

$$Q(t) = \sum_1^N m_i \cdot c \cdot (T_i(t) - T_i^i) \quad (6.3)$$

$$Q(t) = m \cdot c \cdot \sum_1^N 27 \frac{(T_i(t) - T_i^i)}{27} \quad (6.4)$$

$$Q(t) = m \cdot c \cdot N \left[ \sum_1^N \frac{T_i(t)}{N} - \sum_1^N \frac{T_i^i}{N} \right] \quad (6.5)$$

$$Q(t) = m \cdot c \cdot N \cdot (T_a(t) - T_a^i) = N \cdot c \cdot m \cdot \Delta T_a(t) = c \cdot \rho \cdot V \cdot \Delta T_a(t) \quad (6.6)$$

Imposing the same variation of the average temperature in each test you have the same energy<sup>7</sup> given to the system. We tried imposing a variation of  $1.5^\circ C$  and we obtained optimal results using this method.

## 6.6 Calibration of the current sensor

We tested the current sensor with all the configurations to calibrate it. We measured the current as a function of motor velocity.

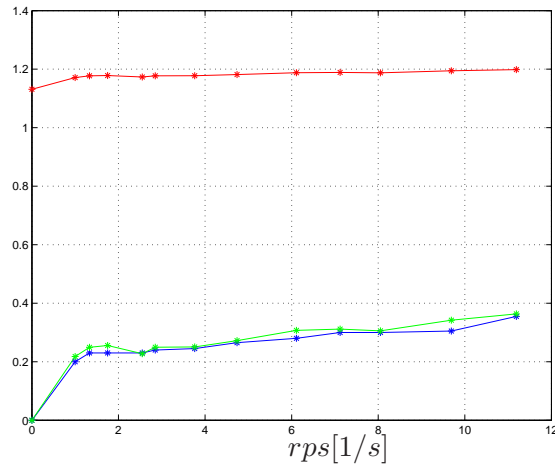


Figure 6.22: Current on rps for free slinky+

<sup>7</sup>approximately 35800J

In figure 6.22 the red line is the voltage output of the current sensor ( $i_s$  [V]), the blue one is the value of the power supply current ( $i_p$  [A])<sup>8</sup>. We knew that this sensor has a sensitivity of 185 mV/A and so we calculated the green line that is the value of measured current ( $i_m$  [A]).

We calculated similar curves for the other three configurations.

## 6.7 Estimation errors

We qualified the mixer measuring these characteristics:

- mixing time
- electric power consumption
- energy consumption

**Mixing time** We calculate the start of the mixing time using the motor data which were acquired at a rate of 1KHz which means a negligible error of 0.001 s. The end of the mixing was found studying the *STD*. Temperatures were acquired at a rate of 3Hz. In the equation of *STD* we used the values of  $T_i^f$ ,  $T_i(t)$  and  $T_a^f$ . It is supposed that the average temperature has not time error because of its stability.  $T_i^f$  and  $T_i(t)$  has the same error time in fact  $T_i^f = T_i(t_{end})$ . We assumed that the total error of mixing time was  $\frac{2}{3}s$ .

**Electric power consumption** We calculated the electric power consumption as the product of the voltage and current of the motor. The relative error of the current is 1.5%<sup>9</sup>. We assumed that the voltage error is 0.01V as the least step of the power supply.

$$\frac{\Delta W}{W} = \frac{\Delta i_m}{i_m} + \frac{\Delta V_m}{V_m} + \frac{\Delta i_m \Delta V_m}{W} \quad (6.7)$$

**Energy consumption** We calculated energy consumption as the product of the mixing time and the electric power consumption.

$$\frac{\Delta E}{E} = \frac{\Delta W}{W} + \frac{\Delta t_m}{t_m} + \frac{\Delta W \Delta t_m}{E} \quad (6.8)$$

The main part of the error came from the error of the  $t_m$ . When it decreases its relative error increases.

---

<sup>8</sup>read directly on the power supply

<sup>9</sup>from the data-sheet of the ACS712



# Chapter 7

## Experimental Data

### 7.1 Case 1: free slinky+

The first configuration we studied is the slinky+. We made several tests with this configuration to validate the experimental setup. The movement of the slinky present different characteristics according to the rotational speed. At low rpm it looked like an helical impeller because it had only rotational velocity. At high velocity it reached its low end because of lift. In the mid range it had a very complex movement: it rotated and moved axially in the cylinder.

We tested the mixer with these value of  $V_m : (1,2,3,4,5,6,7,8)V$ . Finally we used these values  $(1.30,9.5,11)V$  to improve the graph of  $t_m$ .

We decided to implement a simple system to acquire the  $rps$  real-time to control the motor before every test. When we finished all the tests we had the set of  $rps$  to test the other configurations.

$rps$	$t_m$	$W_m$	$E$	$\Delta W/W$	$\Delta E/E$
0.53	316.67	0.2177	68.93	0.0055	0.0371
0.70	163.67	0.3314	54.24	0.0075	0.0391
1.09	55.44	0.4471	24.78	0.0093	0.0601
1.78	29.34	0.5794	16.99	0.0110	0.0816
2.05	28.84	0.7110	20.50	0.0132	0.0748
2.83	34.83	0.9421	32.81	0.0167	0.0577
3.66	23.25	1.2901	29.99	0.0221	0.0688
4.83	20.34	1.8764	38.15	0.0313	0.0677
5.64	14.67	2.2168	32.50	0.0364	0.0835
6.51	13.17	2.4588	31.96	0.0400	0.0897
7.95	14.50	3.3123	48.02	0.0532	0.0770
9.28	14.50	4.0689	58.99	0.0647	0.0743

Table 7.1: Mixing data of slinky+

**Mixing time** As can be seen from figure 7.2 the mixing time has a logarithmic behaviour. At low speed it is quite big and this means that mixer is not working properly. It decreases rapidly with the velocity and reaches an asymptotic value of 14s.

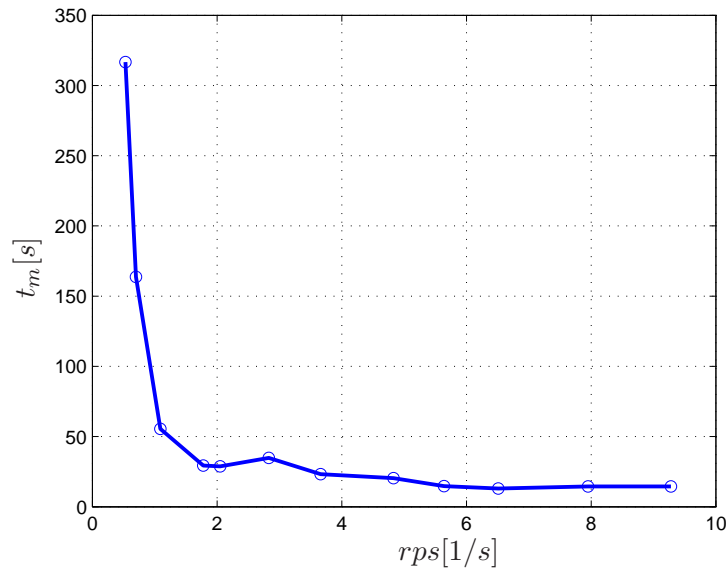


Figure 7.1:  $t_m$  of slinky+

**Electric power consumption** The electric power consumption grows linearly with the velocity (fig. 7.4). The minimum value is  $0.2177W$  and the maximum is  $4.0689W$ .

**Energy consumption** The high value of the  $t_m$  at low speed makes the energy consumption big. Increasing the velocity the energy decreases to a minimum of  $16.99J$  at  $1.78rps$ . The maximum value is  $68.93J$  at  $0.53rps$ . The maximum measured relative error is  $8.97\%$  at  $6.51rps$ . It's interesting because it has three minima, two of which relative.



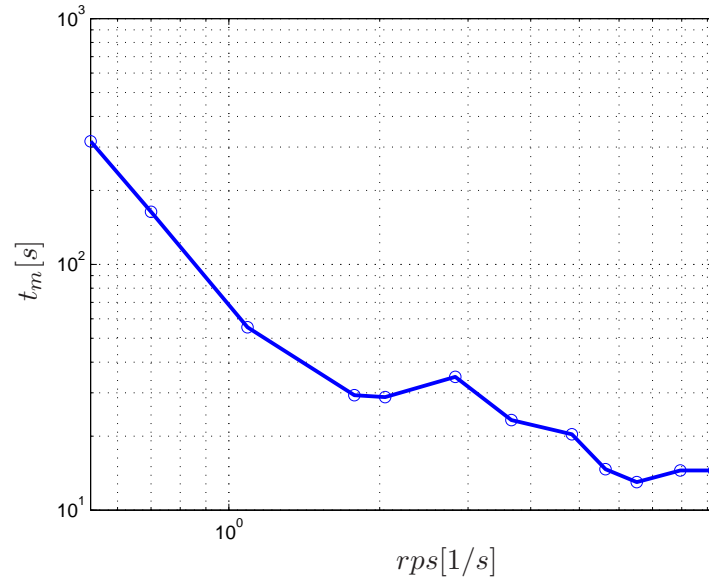
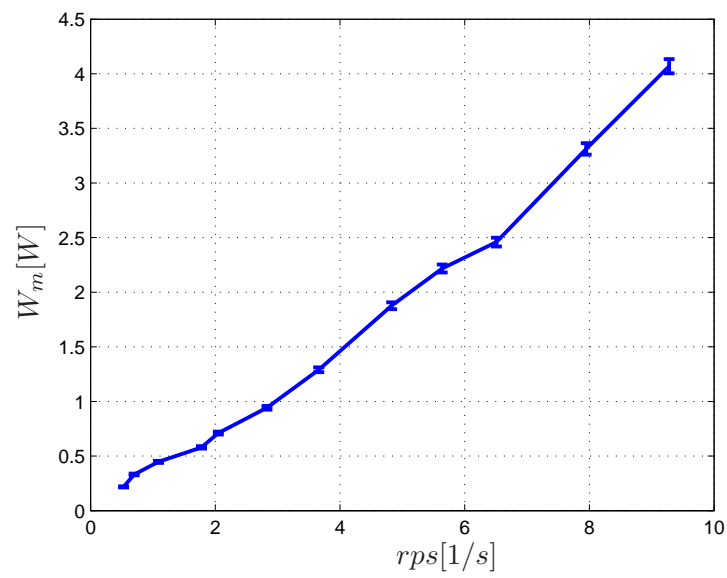
Figure 7.2: Logarithmic graph of  $t_m$  of slinky+

Figure 7.3: Electric power consumption of slinky+

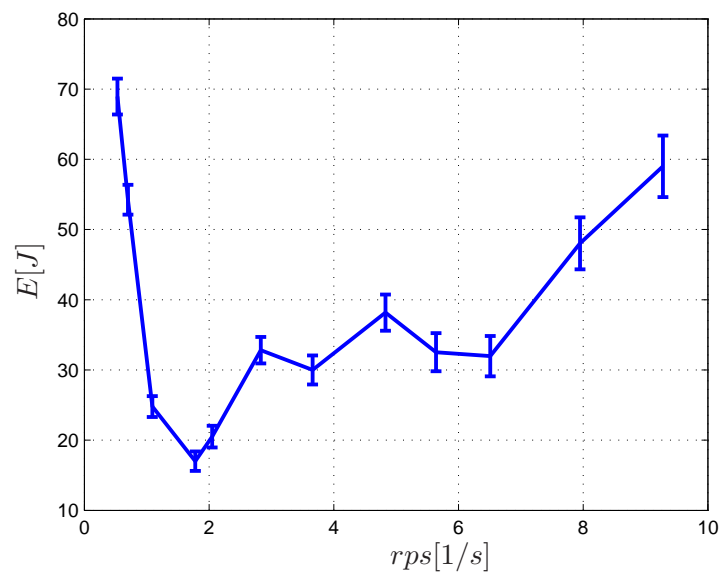


Figure 7.4: Energy consumption of slinky+

## 7.2 Case 2: free slinky-

We inverted the power wires to change the rotational sense of the motor. The behaviour of the slinky is the same as the previous set of tests with some differences at high velocities. At high velocity it reaches its high end. In the mid range it shows the same behaviour of the first configuration.

We tested this configuration following the velocities of previous tests. As we supposed we had slightly different values of power and voltage.

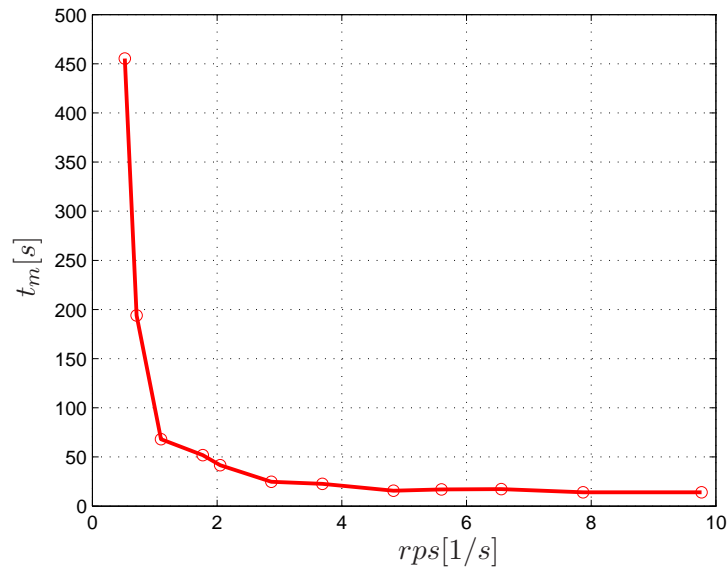
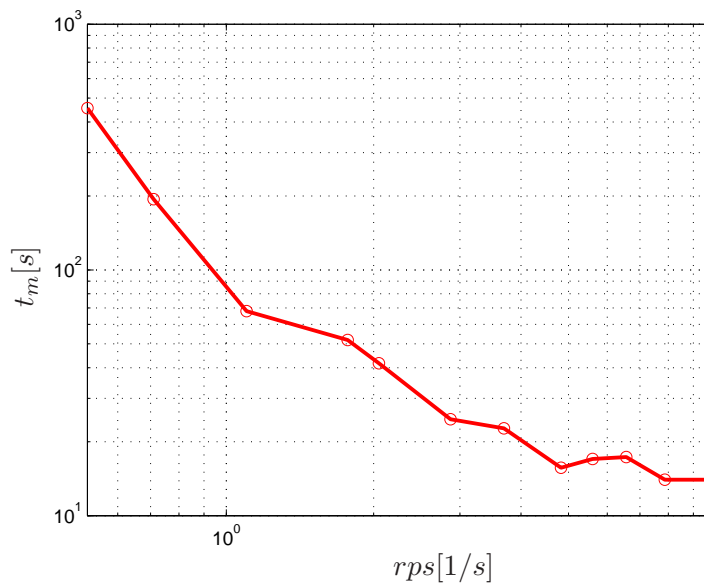
$rps$	$t_m$	$W_m$	$E$	$\Delta W/W$	$\Delta E/E$
0.52	455.33	0.1890	86.05	0.0047	0.0341
0.71	194.00	0.2397	46.50	0.0055	0.0408
1.10	68.00	0.3643	24.77	0.0075	0.0576
1.77	51.84	0.5622	29.14	0.0107	0.0551
2.05	41.67	0.6435	26.81	0.0119	0.0598
2.87	24.67	0.9669	26.14	0.0170	0.0733
3.69	22.67	1.3964	31.65	0.0239	0.0683
4.83	15.67	1.6686	26.14	0.0278	0.0858
5.60	17.00	1.9883	33.80	0.0327	0.0764
6.56	17.33	2.4749	42.89	0.0402	0.0712
7.87	14.00	3.1957	44.74	0.0513	0.0797
9.77	14.00	4.2663	59.73	0.0676	0.0758

Table 7.2: Mixing data of slinky-

**Mixing time** The mixing time has a logarithmic behaviour as can be seen in figure 7.6. At low speed it is, once again, quite big. It decreases rapidly with the velocity and reaches an asymptotic value of 14s.

**Electric power consumption** As before, the electric power consumption is a linear function of the velocity (fig. 7.8). The minimum value is 0.1890W and the maximum is 4.2663W.

**Energy consumption** The high value of the  $t_m$  at low speed makes the energy consumption big (fig. 7.7). Increasing the velocity the energy decreases to a minimum of 24.77J at 1.10rps. The maximum value is 86.05J at 0.52rps. The measured maximum value error is 8.58% at 4.83rps.

Figure 7.5:  $t_m$  for slinky-Figure 7.6: Logarithmic graph of  $t_m$  of slinky-

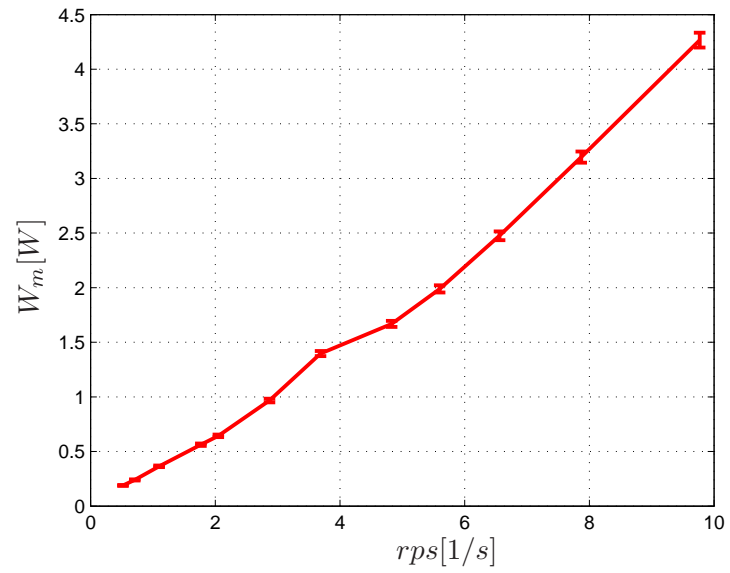


Figure 7.7: Electric power consumption of slinky-

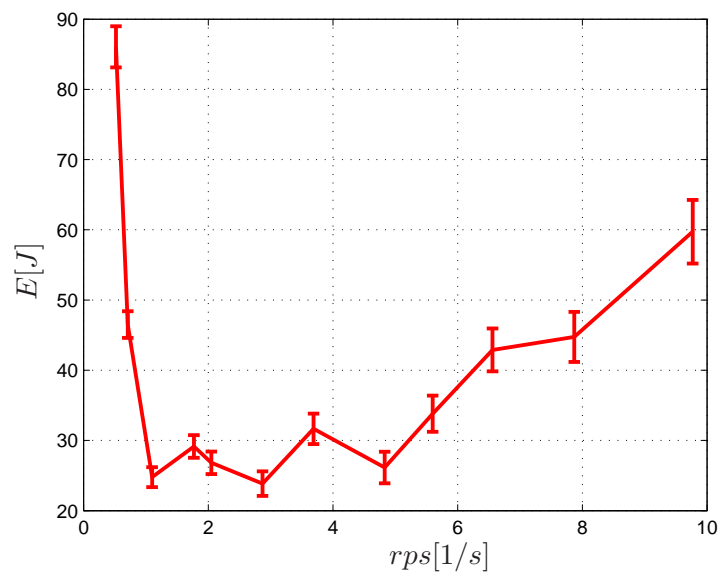


Figure 7.8: Energy consumption of slinky-



### 7.3 Case 3: fixed slinky

We decide to fix the slinky to avoid axial movements. This is a simple test to verify the influence of the described movements on the performance of the mixer. We used some plastic cable ties to fix the slinky to the shaft.

We tested the mixer at the following velocities.

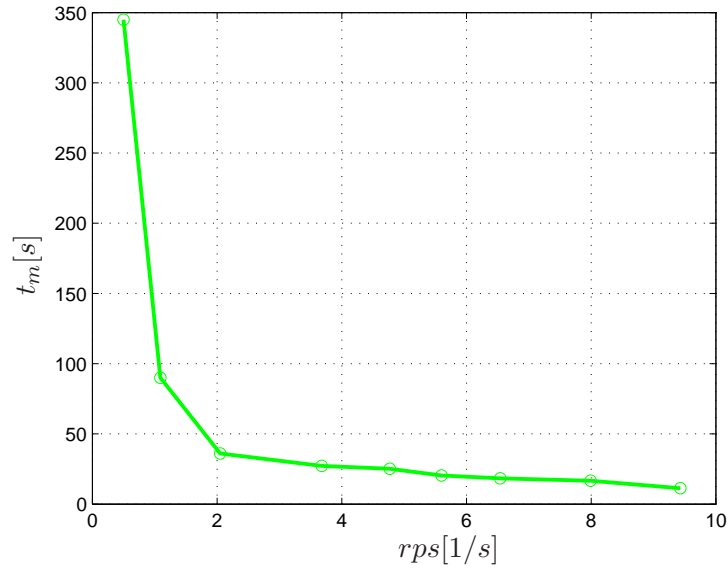
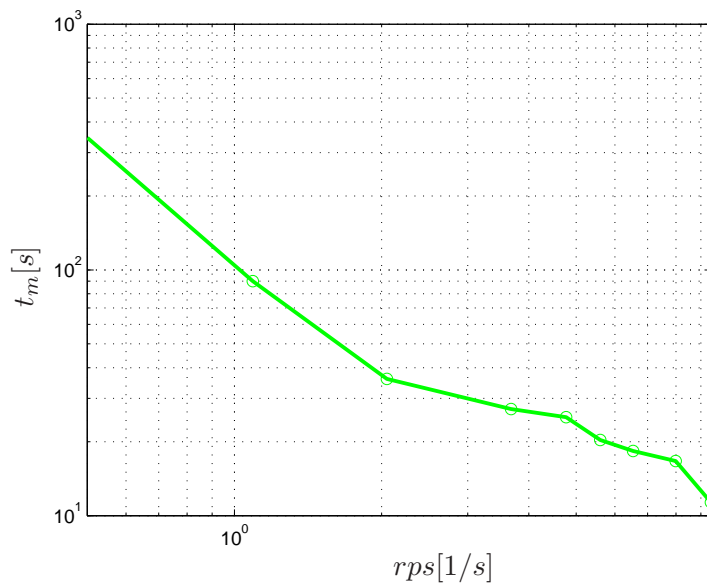
$rps$	$t_m$	$W_m$	$E$	$\Delta W/W$	$\Delta E/E$
0.50	345.00	0.2545	87.80	0.0062	0.0340
1.09	90.00	0.4580	41.22	0.0093	0.0441
2.05	36.00	0.7448	26.81	0.0137	0.0623
3.68	27.17	1.4490	37.19	0.0247	0.0591
4.77	25.17	2.0477	51.54	0.0340	0.0567
5.60	20.33	2.4034	48.86	0.0394	0.0636
6.54	18.33	2.9978	54.94	0.0486	0.0656
7.99	16.67	3.6686	61.15	0.0588	0.0679
9.43	11.33	5.1047	57.83	0.0810	0.0876

Table 7.3: Mixing data of fixed slinky

**Mixing time** In this configuration the mixing time decrease logarithmicly as in the the other tests (fig. 7.10). At low speed, once again, the mixer is not working properly. It decreases rapidly as the velocity increase.

**Electric power consumption** As previous tests the electric power consumption depends linearly on the velocity (fig. 7.12). The minimum value is  $0.2545W$  and the maximum is  $5.1047W$ .

**Energy consumption** At low speed the energy consumption is big (fig. 7.11) because of the high value of  $t_m$ . Increasing the velocity the energy decreases to a minimum of  $26.81J$  at  $2.05rps$ . The maximum value is  $87.80J$  at  $0.50rps$ . The measured relative error increased with velocity and its maximum value is  $8.76\%$  at  $9.43rps$ .

Figure 7.9:  $t_m$  for fixed slinkyFigure 7.10: Logarithmic graph of  $t_m$  of fixed slinky



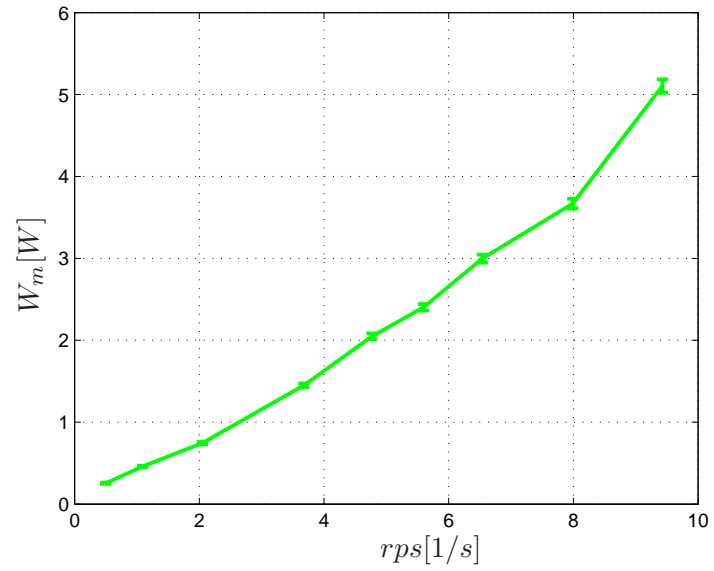


Figure 7.11: Electric power consumption of fixed slinky

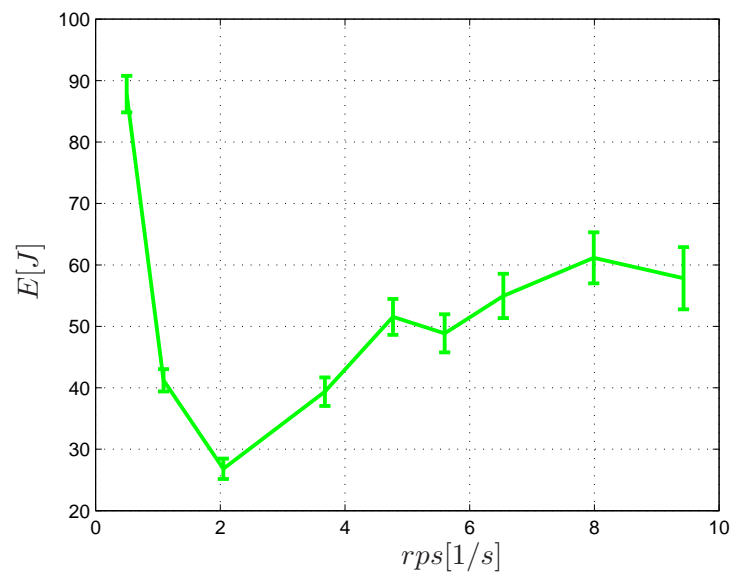


Figure 7.12: Energy consumption of fixed slinky



## 7.4 Case 4: impeller

After the tests with the slinky we mounted an impeller on the shaft. We decided to make the initial tests with an impeller taken from an old pc fan. It was ideal to create the axial flow field needed because of the height ratio  $H/D$  of the mixer.

We tested the mixer following the velocities of previous tests with some limitations at high velocities.

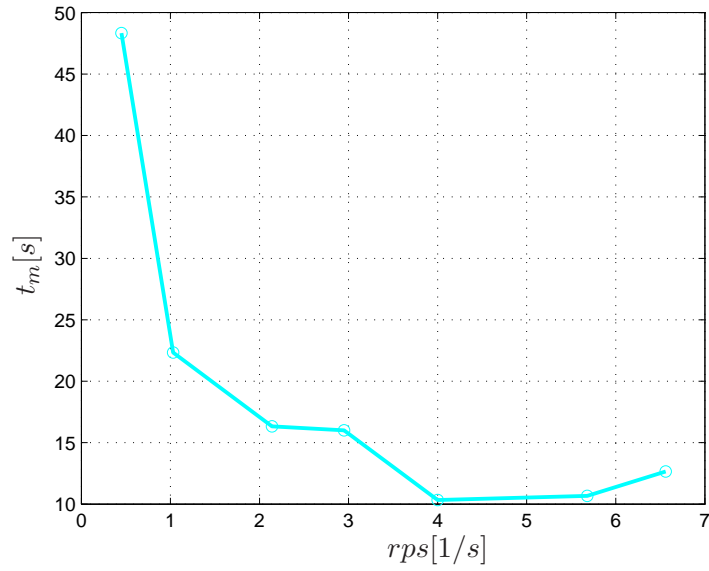
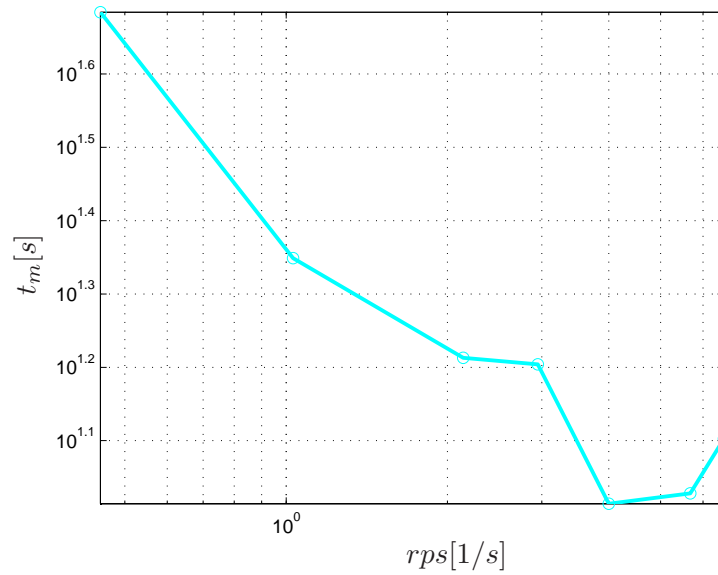
$rps$	$t_m$	$W_m$	$E$	$\Delta W/W$	$\Delta E/E$	$Re[10^4]$
0.45	48.33	0.3020	14.59	0.0071	0.0835	0.6480
1.03	22.33	0.5268	11.59	0.0106	0.1076	1.4832
2.14	16.33	0.8024	13.10	0.0146	0.1110	3.0816
2.95	16.00	1.6084	25.73	0.0280	0.0861	4.2480
4.00	10.33	3.7958	39.21	0.0634	0.0999	5.7600
5.68	10.67	6.6813	71.22	0.1081	0.0895	8.1792
6.56	12.66	10.4435	132.21	0.1670	0.0750	9.1164

Table 7.4: Mixing data of impeller

**Mixing time** Also in this case the mixing time has a logarithmic behaviour as can be seen in figure 7.14. At low speed it is significantly smaller than in the others configurations. It decreases with the velocity.

**Electric power consumption** The electric power consumption is an exponential function of the velocity (fig. 7.15). Its minimum value is  $0.3020W$  and the maximum is  $10.4435W$ .

**Energy consumption** The high value of the  $W_m$  at high velocities results in an higher power consumption (fig. 7.16). The energy has a minimum of  $11.59J$  at  $1.03rps$ . The maximum value is  $132.21J$  at  $6.56rps$ . In the condition of best efficiency it has a relative error of 10.76%.

Figure 7.13:  $t_m$  for impellerFigure 7.14: Logarithmic graph of  $t_m$  for impeller

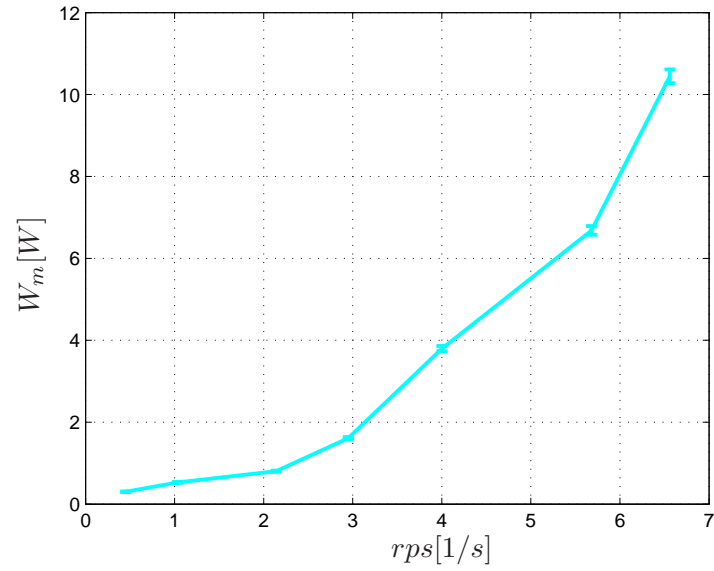


Figure 7.15: Electric power consumption of impeller

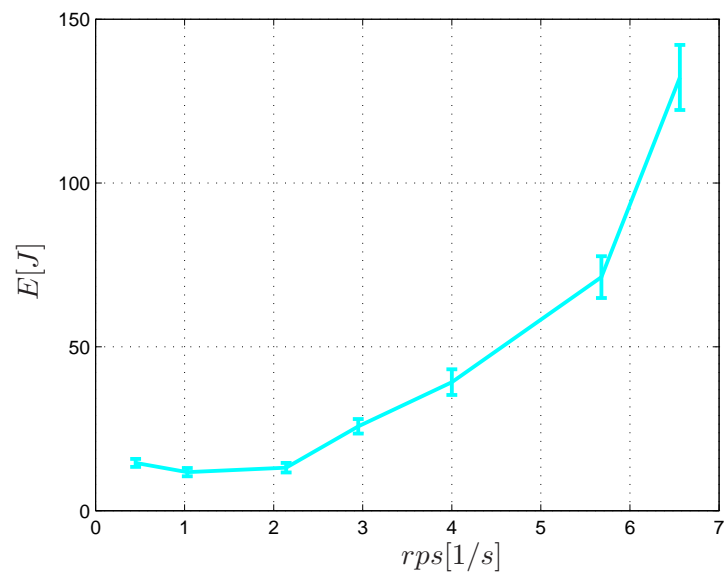


Figure 7.16: Energy consumption of impeller



## 7.5 Comparison

The aim of this work was to qualify this kind of new mixer. The comparison of the different configurations shows some interesting elements.

**Mixing time** The  $t_m$  of the impeller is always smaller than the  $t_m$  of other configurations at every velocity (fig. 7.17).

**Electric power consumption** At low velocities there are not differences between various configurations. After  $3rps$  the  $W_m$  of the impeller increases exponentially and becomes three times higher than the value of the slinky configurations  $W_m$  (fig. 7.19). We stopped before  $7rps$  because the power request exceeded the capabilities of our power supply. This increase was probably caused by hydrodynamic resistance.

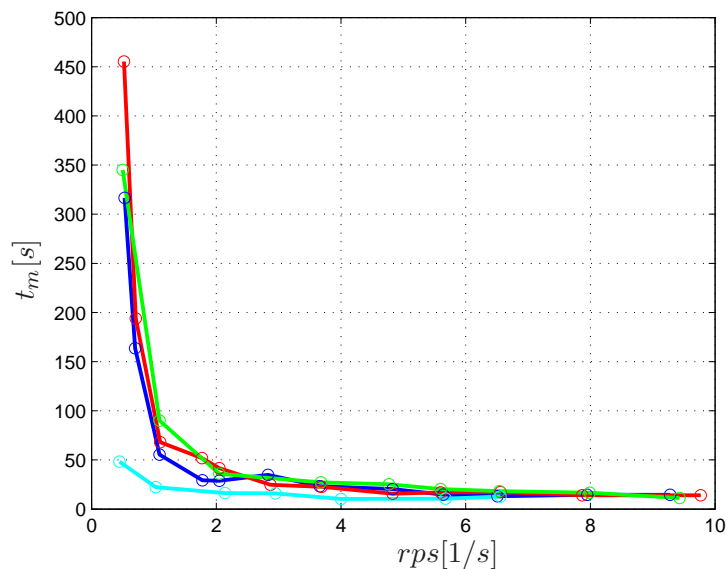


Figure 7.17: Comparison of  $t_m$

**Energy consumption** This graph is probably the most useful piece of information of this work (fig. 7.20). You can see that the fixed slinky is worse than both the free slinky configurations. So we can say that the axial movements of the spring reduce the energy consumption. The slinky reaches higher velocities than the impeller thanks to its smaller power consumption.

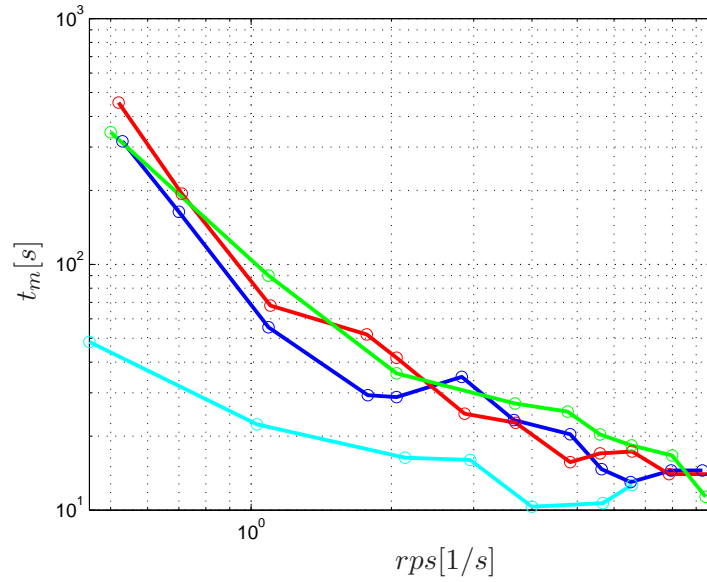
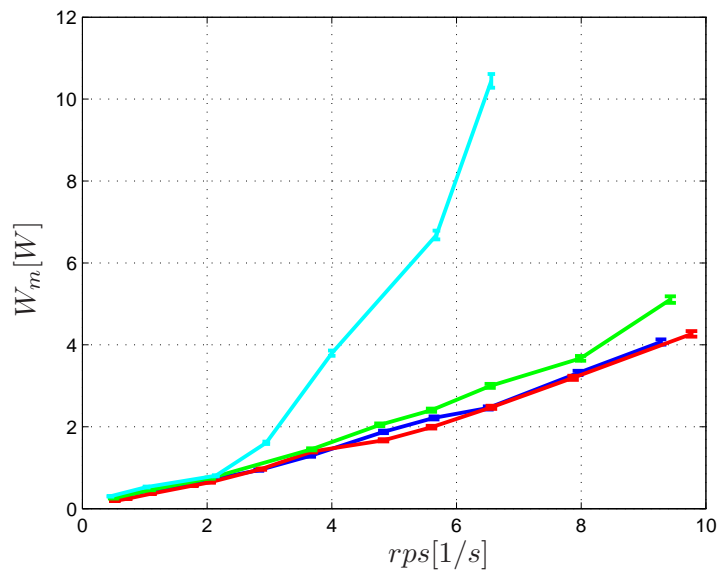
Figure 7.18: Logarithmic graph of comparison of  $t_m$ 

Figure 7.19: Comparison of electric power consumption



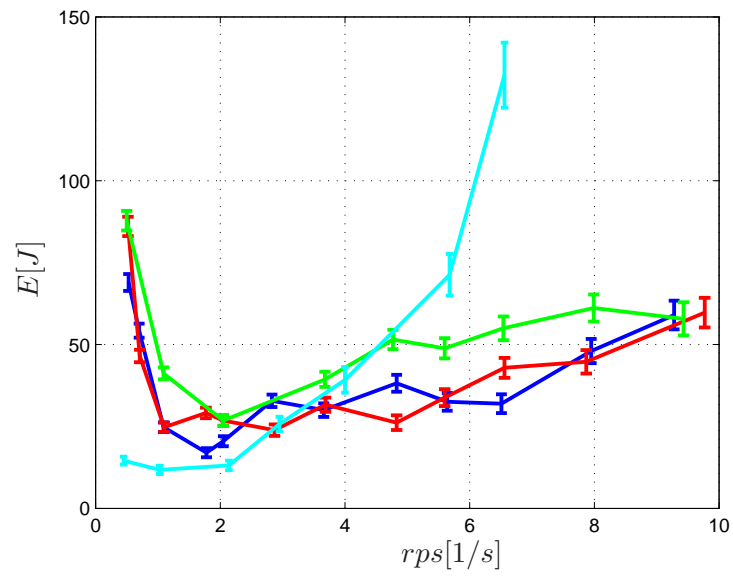


Figure 7.20: Comparison of energy consumption



## Chapter 8

# Conclusions

### 8.1 Achievements

The present work was entirely developed in the thermofluid dynamics laboratory of the University of Studies of Brescia. The aim of this dissertation was the study of an unconventional turbulent mixer and compare it with a classic impeller configuration. We tested the mixer performance using measures of temperature and mix water at different temperatures.

The first point of the work was the design and the construction of the mixer. We tried to create a versatile structure that could be improved during the work. The mixer that we created is composed by few parts that can be easily replaced if necessary. In this way mixer could be used in different tests.

The second step was to add temperatures sensors and a heat exchanger system. We placed twenty-seven thermocouples along the height of the mixer. Knowing the temperatures of every layer of the mixer allowed us to have useful informations to do more complete tests. Preliminarily we used a thermostatic bath to cool the bottom of the water to test the sensors' system. In main tests we used a resistor as heating system to heat the top layer of the cylinder. Using a heating system instead of a cooling system allowed us to make faster tests.

Finally we developed an experimental procedure to make the measures we were looking for: mixing time and electric power consumption. We used the velocity as reference for each test. We tested four different configurations. None of the configurations has been optimized because of the great number of tests necessary to qualify the systems.

The results of the experiments are satisfactory. In every configuration trend of the mixing time as a function of the rotation speed is a logarithmic type in agreement with the literature (fig. 7.18). The configuration equipped with impeller presents mixing times lower but an electric power consumption higher than the one with spring. In terms of energy consumption, the propeller system is efficient at low speeds, the spring is efficient at high speeds (fig. 7.20).

Results of this work permitted us to make some important considerations. All the measures of the mixing time were made as function of velocity, so you can

use another motor to make the same measures. The measures of electric power consumption were done in succession after all the tests. These results don't say the real power consumption for mixing but the consumption of the motor we used in our tests. They can be used to compare different configurations.

## 8.2 Future developments

This work demonstrated the feasibility of a mixer equipped with slinky spring for mixing liquids and justifies possible future searches for a better understanding of the dynamics of the mixing taking place in it.

All the data acquired in these tests could be analysed to find some other informations. For example you can study which thermocouples are relevant to describe the mixing making a statistical work or you can calculate the mixing time with smaller or greater degree of homogeneity.

It would be interesting to make some visualization tests, like Mavros in [10], to understand the variation of the flow field caused by the slinky movement. This knowledge could enable us to use a little number of sensors.

You can qualify a mixer by measuring degree of mechanical damage. This is a very important factor in a lot of mixing processes (as shown by Papoutsakis in [7]). It is supposed that little electric power consumption of the slinky is caused by a smaller mechanical damage than the system with the impeller.

The final step could be development of a campaign of tests to optimize the mixer.



## Notations

$c$	specific heat
$D$	diameter of the impeller
$D_c$	diameter of the mixer cylinder
$E$	energy consumption
$H$	height of the cylinder
$m_i$	mass of i-th layer
$N$	number of thermocouples
$N_i$	number of i-th thermocouple
$N_t$	dimensionless mixing time
$i_m$	measured current
$i_p$	power supply current
$i_s$	output of the current sensor
$Q$	heat
$Re$	Reynolds number
$rps$	round per seconds
slinky+	free slinky that moves counter-clockwise
slinky-	free slinky that moves clockwise
$STD$	standard deviation
$t_{end}$	final time of a test
$t_m$	mixing time
$T_a^i$	initial average temperature
$T_a^f$	final average temperature
$T_i^i$	initial temperature of i-th thermocouple
$T_i^f$	final temperature of i-th thermocouple

$T'$	derivative on time of temperature
$V$	volume of the cylinder
$V_{cc}$	supply voltage
$V_m$	motor voltage
$W_m$	electric power consumption
$\alpha$	thermal diffusivity
$\Delta i_m$	measured current error
$\Delta V_m$	motor voltage error
$\Delta W$	electric power consumption error
$\Delta T_i^f$	difference between $T_i^f$ and $T_a^f$
$\Delta T_i^{tot}$	difference between $T_a^i$ and $T_a^f$
$\lambda$	thermal conductivity
$\mu$	dynamic viscosity
$\rho$	density





# Bibliography

- [1] F. Ippolito F. Scargliati A. Brucato A. Busciglio, F. Grisafi. Mixing time in unbaffled stirred tanks. In *14<sup>th</sup> European Conference on Mixing*, 2012.
- [2] Dassault Systemes SolidWorks Corporation, 300 Baker Avenue, Concord, MA 01742 USA. *Guida dello studente per l'apprendimento del software SolidWorks*.
- [3] Suzanne M. Kresta Edward L. Paul, Victor A. Atimeo-Obeng. *Handbook of industrial mixing : science and practice*. Wiley Interscience, 2004.
- [4] Ivan Fort and Tomas Jirout. A study on blending characteristics of axial flow impellers. *Chemical and Process Engineering*, 32:311–319, 2011.
- [5] Hans-Petter Halvorsen. Data acquisition in labview, 2011.
- [6] John H. Lienhard IV John H. Lienhard IV. *A heat transfer textbook*. Phlogiston Press, third edition, 2008.
- [7] Eleftherios T. Papoutsakis. Fluid-mechanical damage of animal cells in bioreactor. *Tibtech*, 9:427–437, 1991.
- [8] Aniruddha B. Pandit Parag R. Gogate, Anthony A.C.M. Beenackers. Multiple-impeller systems with a special emphasis on bioreactors: a critical review. *Biochemical Engineering Journal*, pages 109–144, 2000.
- [9] Francesco Pasqua. Analisi sperimentale preliminare di un dispositivo innovativo per il mixing turbolento, 2011.
- [10] P. Mavros. Flow visualization in stirred vessels - a review of experimental techniques. *Trans IChemE*, 79:113–127, 2001.
- [11] I. Fort T. Jirout F. Riege R. Allner R. Sperling. Study of the blending efficiency of pitched blade impellers. *Acta Polytechnica*, 41(6):7–13, 2001.



## Ringraziamenti

Innanzitutto ringrazio i professori Maurizio Quadrio e Pietro Poesio per l'opportunità che mi hanno concesso nel realizzare questo lavoro di tesi. Entrambi sono sempre stati disponibili ad aiutarmi nel mio cammino.

Merito di questa ricerca va anche, e direi soprattutto, al dottorando Stefano Farisè che mi ha assistito fin dall'inizio di questa mia avventura all'università di Brescia. Non c'è stato giorno in cui non mi abbia insegnato qualcosa di nuovo e mi sento molto fortunato di aver condiviso il suo ultimo anno da dottorando.

Ringrazio tutti i ragazzi dei laboratori di Brescia, in particolar modo l'ing. Marco De Mori per le continue assistenze in ambito elettronico.

Ringrazio la mia famiglia per il continuo supporto che mi ha dato in questi anni. I miei genitori che sono sempre stati un esempio per me. Mia sorella che, in ogni occasione, è stata pronta ad aiutarmi, sin dall'inizio della mia carriera universitaria. Mio fratello che non ha mai smesso di credere nelle mie capacità. I miei nipoti che riescono sempre a tirarmi su di morale. I miei zii per avermi incoraggiato. Zio Elio che mi ha insegnato cosa significhi essere un bravo zio. Zia Lia sempre pronta a chiamarmi per sapere come andavano le cose. Zia Gina che nonostante la lontananza riesce sempre a farsi sentire vicina. Tutti i miei cugini, in particolar modo Fabiana.

Vorrei ringraziare tutti i miei compagni di università. Finito questo percorso potrò chiamarli per quello che sono diventati, degli amici insostituibili. Primo fra tutti Alain che dopo tutto questo tempo ormai è diventato come un secondo fratello. Francesco con cui ho condiviso la mia passione per il mondo automobilistico. Marco che mi ha sopportato a lungo durante i viaggi in treno. Matteo sempre pronto a confrontarsi durante le sessioni di studio. Il gruppo dei Dronisti con cui ho passato un piacevole anno. Infine tutti gli altri compagni di università.

Ringrazio tutti i miei amici che non vedevano l'ora che arrivasse questo momento. I miei migliori amici, Alice e Giovanni. La prima per le continue uscite a chiacchiere, il secondo perchè non esistono persone come lui. Andrea per le serate passate a filosofeggiare. Fabio sempre pronto ad offrirmi un caffè e fare due chiacchiere. Dan con cui ho condiviso molte sessioni di studio. Stefano, Giuseppe, Dorina e tutti gli altri amici.

Infine ringrazio tutte le persone che ho avuto modo di conoscere in questi anni di università e che mi hanno aiutato a crescere.